ResearchGate

See discussions, stats, and author profiles for this publication at: https://www.researchgate.net/publication/47531130

Proteomics and Transcriptomics Investigation on longissimus Muscles in Large White and Casertana Pig Breeds

ARTICLE *in* JOURNAL OF PROTEOME RESEARCH · OCTOBER 2010

Impact Factor: 4.25 · DOI: 10.1021/pr100693h · Source: PubMed

CITATIONS
33

READS
95

8 AUTHORS, INCLUDING:

Alessandra Crisà
CREA Agricultural Research Council
34 PUBLICATIONS **254** CITATIONS
SEE PROFILE

Gianluca Prosperini
CONSORZIO INTERUNIVERSITARIO PER LE …
8 PUBLICATIONS **98** CITATIONS
SEE PROFILE

Anna Maria Timperio
Tuscia University
85 PUBLICATIONS **1,459** CITATIONS
SEE PROFILE

Alessio Valentini
Tuscia University
117 PUBLICATIONS **1,652** CITATIONS
SEE PROFILE

Available from: Angelo D'Alessandro
Retrieved on: 31 January 2016

research articles Journal of proteome research

Proteomics and Transcriptomics Investigation on *longissimus* Muscles in Large White and Casertana Pig Breeds

Leonardo Murgiano,[†] Angelo D'Alessandro,[‡] Maria Giulia Egidi,[‡] Alessandra Crisà,[†] Gianluca Prosperini,[†] Anna Maria Timperio,[‡] Alessio Valentini,[†] and Lello Zolla*[,‡]

Dipartimento di Produzioni Animali, Università della Tuscia, Via de Lellis, 01100 Viterbo, Italy, and Dipartimento di Scienze Ambientali, Università della Tuscia, L.go dell'Università snc, 01100, Viterbo, Italy

Received July 6, 2010

Consumer complaints against the blandness of modern lean meat and the frequent reference to the more strongly flavored meat that was available years ago have prompted reconsideration of high fat-depositing typical pig breeds. Casertana and Large White pig breeds are characterized by a different tendency toward fat accumulation as they exhibit opposite genetic and physiological traits with respect to the energy metabolism. These physiological differences were investigated in *longissimus lumborum* muscles through proteomics (2-DE, MS/MS) and microarray approaches. Data were analyzed for pathway and network analyses, as well as GO term enrichment of biological functions. As a result, Casertana showed a greater amount of proteins involved in glycolitic metabolism and mainly rely on fast-mobilizable energy sources. Large White overexpressed cell cycle and skeletal muscle growth related genes. Metabolic behavior and other implications are discussed.

Keywords: Casertana pig breed • Large White pig breed • fat deposition • interactomics • proteomics • microarray

Introduction

Europe and China are the origin of about 70% of breed diversity in the world.[1] In both China and Europe, pig has been and remains a major meat producer. Molecular approaches to improve pig meat quality have been rapidly emerging and gaining momentum,[2] especially those kinds of investigations that are oriented toward comparisons between different breeds through integrated proteomics and transcriptomics analyses.[3,4]

Europe has 228 listed existing breeds, plus 105 now extinct; China has 118 listed breeds and 10 more extinct as it has been reported in the World Watch List for Domestic Animal Diversity.[5] In the late 18th century, many new pig breeds, such as the Large White (LW) and the Berkshire in the U.K., came into existence and were distributed globally to replace or improve local breeds.[6] Indeed, many of the European local breeds have been heavily altered and three-quarters of local or traditional breeds are extinct or marginalized. This is the case of the black pigs of Italy, which have been long questioned to be influenced by pigs imported from China—although it is still controversial, as they appear to be closely related to the Iberian groups[1] or rather belong to an independent area of domestication on the Italian peninsula, which is opposed to the rest of Europe.[7] Italian black pigs might date back to Roman times or, more likely, to the 17th century.[8] One Italian breed in particular, the Neapolitan, played a pivotal role in the formation of some of the English breeds such as the Berkshire and the Large Black.[1] The Casertana (CA) and Calabrese directly descend from the Neapolitan lineage, which is formally extinct. Casertana is an endangered pig breed, very ancient and absolutely singular. It has been raised for centuries in semiwild conditions in the forests near Caserta and Benevento, where it fed on acorns, chestnuts and other vegetables of the bush.

CA and LW exhibit an opposite genetic profile with respect to the energy metabolism. Chemical composition of muscles from CA and its crossbreeds (also with LW) has already been investigated,[9] underlying that CA muscles are characterized by a higher lipid content and a lower protein content. Zullo et al. reported that CA and Landrace × (Landrace × LW) pigs provided a product with the lowest chewing value; moreover, CA × (Landrace × LW) pigs produced meat with the highest water holding capacity, while CA pigs produced lighter commercial cuts.[9] Studies with CA pigs may shed light on the physiological process of fat deposition because these animals are prone to adipogenesis and have a strong aptitude for fat deposition. Indeed, CA pigs have a higher percentage of body fat and produce more than double backfat thickness as LW pigs.[10] Since this breed did not undergo selection programmes, CA pigs retain the traits of a slow growing and high fat depositing pig compared to the genetic lines actually exploited in the pig industry. Comparison with LW pigs demonstrated that the CA is far less competitive regarding growth performance, reaching a commercial slaughter weight at a considerably greater age, and with a 2-fold increase in backfat thickness.[10]

Skeletal muscle is a heterogeneous tissue that is made up of several fiber types.[11] These compositional differences deter-

* To whom correspondence should be addressed. Lello Zolla. E-mail: zolla@unitus.it. Tel.: +39 0761 357100. Fax: +39 0761 357179. L.go dell'Università snc, University of Tuscia, 01100 Viterbo (VT), Italy.
[†] Dipartimento di Produzioni Animali.
[‡] Dipartimento di Scienze Ambientali.

10.1021/pr100693h
© 2010 American Chemical Society
Published on Web 10/22/2010

mine distinct metabolic and physiological functions and affect body composition as well as meat quality.[12,13] Muscles are traditionally distinguished among slow-twitch oxidative, fast-twitch glycolytic/oxidative (red muscles) and fast-twitch glycolytic only (white muscles).[14]

Red muscles (for example *soleus* and *psoas*) are adapted to undertake chronic contractile activity without fatigue under aerobic respiratory conditions and are characterized by a higher percentage of capillaries, myoglobin, lipids and mitochondria than white skeletal muscles.

On the other hand, white muscles, such as the *gastrocnemius* and *longissimus lumborum*, are recruited sporadically during the brief periods of intense muscular activity.[3,6] White and red muscles also differ in their fiber type composition.

A preliminary proteomics portrait of the *longissimus lumborum* muscle has been recently provided, mainly aiming at determining the molecular characteristics influencing meat quality, on the basis of a comparative analysis on the role of alternative genetic backgrounds.[15,16]

The proteome analysis based on 2-DE and mass spectrometry is a method of choice for the quantitative differential display of large numbers of proteins and is a promising and powerful tool in meat science. Differential proteomics analyses between different pig breeds have already been performed (Meishan vs LW, Pietrain vs Duroc × (LW × Hampshire)).[3,4]

In the present study, we performed proteomics, transcriptomics and interactomics network/pathway analyses, along with functional enrichment of GO terms, to the end of characterizing and comparing expression profiles in the *longissimus lumborum* of CA and LW. Our aim was to reveal the differences of breed-related protein/transcript expression patterns between the CA and the LW. These observations might be useful to deepen our understanding of the genetic differences among these breeds, as well as the molecular mechanisms responsible for breed-specific peculiar growth performance.

Materials and Methods

Sample Collection. All animals used in this study were treated according to International Guiding Principles for Biomedical Research Involving Animals. In a commercial dairy farm located in Viterbo (Italy), we selected 20 animals (10 per breed) which were of the same age and fed the same diet.

Proteomic Analysis. Sample Preparation. Sample preparation and solubilization was performed by slight modification of the SWISS-2D PAGE sample preparation procedure.[17] Frozen samples of *longissimus lumborum* from 10 LW and 10 CA (approximately 20 mg per sample) were crushed in a mortar containing liquid nitrogen, and to remove lipids, proteins were precipitated from a desired volume of each sample with a cold mix of tri-*n*-butyl phosphate/acetone/methanol (1:12:1). After incubation at 4 °C for 90 min, the precipitate was pelleted by centrifugation at 2800× *g*, for 20 min at 4 °C. After washing with the same solution, the pellet was air-dried and then resuspended in the focusing solution containing 7 M urea, 2 M thiourea, 4% (w/v) CHAPS, 0.8% (w/v) pH 3−10 carrier ampholyte, 40 mM Tris, 5 mM TBP, 0.1 mM EDTA (pH 8.5), 2% (v/v) protease inhibitor cocktail (Sigma-Aldrich, Basle, Switzerland), and 2 mM PMSF. Before focusing, the sample was incubated in this solution for 3 h at room temperature, under strong agitation. Alkylation has been performed with 7.7 mM Iodoacetamide in a solution of 7 M urea, 2 M thiourea, 4% CHAPS, 20 mM Tris, pH 3−10 carrier ampholyte, 40 mM Tris, 5 mM TBP, 0.1 mM EDTA (pH 8.5), 2% (v/v) protease inhibitor cocktail (Sigma-Aldrich). To prevent overalkylation, iodoacetamide excess was destroyed by adding equimolar amount of DTE. The protein concentration of each group was determined according to Bradford[18] using BSA as a standard curve.

Semiquantitative IEF-SDS PAGE. Eight-hundred micrograms of protein were resuspended in 7 M urea, 2 M thiourea, 4% CHAPS, pH 3−10 carrier ampholyte (total volume 250 μL) and then used to rehydrate 18 cm long IPG 3−10 NL (Amersham Biosciences) for 8 h (1 mg of protein each strip). IEF was carried out on a Multiphor II (Amersham Biosciences) with a maximum current setting of 50 μA/strip at 20 °C.[19] IEF was performed using ready-to-use Immobiline Dry-Strips linear pH gradient 3−10 length 18 cm (Biorad, CA, USA) and the in gel sample rehydration method. IEF was run on an Protean IEF BIORAD at 20 °C constant temperature and 8000 V for 99 000 Vh. After IEF, the IPG gel strips were incubated at room temperature for 30 min in 6 M urea, 30% w/v glycerol, 2% w/v SDS, 5 mM Tris-HCl, pH 8.6. The strips were sealed at the top of a 1.0 mm vertical second dimensional gel (Biorad) with 0.5% agarose in 25 mM Tris, 192 mM glycine, 0.1% SDS, pH 8.3. SDS-PAGE was carried out on homogeneous running gels 12% T 3% C The running buffer was 25 mM Tris, 192 mM glycine, 0.1% SDS, pH 8.3 and running conditions were 40 mA/gel until the bromophenol blue reached the bottom of the gel. Molecular weight marker used was Wide Range Weight Electrophoresis Calibration Kit (Amersham Biosciences, U.K.). Gels were automatically stained with Brilliant Blue G colloidal (Sigma, St. Louis, MO) following the manufacturer's instructions. Gels have been destained overnight in deionized water with blotting paper meant to gather Coomassie excess. Three technical replicates per sample were performed.

Image Analysis. Sixty stained gels (3 technical replicates × 10 biological replicates × 2 breeds) were digitalized using an ImageScanner and LabScan software 3.01 (Bio-Rad Hercules, CA). The 2-DE image analysis was carried out and spots were detected and quantified using the Progenesis SameSpots software v.2.0.2733.19819 software package (Nonlinear Dynamics, New Castle, U.K.). Each gel was analyzed for spot detection and background subtraction. Within-group comparison of protein spot numbers was determined by repeated measures analysis. Among-group comparisons were determined by ANOVA (Analysis of Variance) procedure in order to classify sets of proteins that showed a statistically significant difference with a confidence level of 0.05. Spots which were significantly different between groups (LW and CA) and not significantly different in the three technical replicate and ten biological replicate samples were identified by qTOF-MS/MS. All statistical analyses were performed with the Progenesis SameSpots software v.2.0.2733.19819 software package.[20] After the background subtraction, spot detection and match, one standard gel was obtained for each group (Figure 1), LW and CA. These standard gels were then matched to yield information about the spots of differentially expressed proteins. Differential protein expression was considered significant at $P < 0.05$ and the change in the photodensity of protein spots between LW and CA samples had to be more than 2 fold.

In-Gel Digestion. Spots from 2-DE maps of biological interest ($P < 0.05$) were carefully excised from the gel and subjected to in-gel trypsin digestion according to Shevchenko et al.[21] with minor modifications. The gel pieces were swollen in a digestion buffer containing 50 mM NH_4HCO_3 and 12.5 ng/mL trypsin (modified porcine trypsin, sequencing grade,

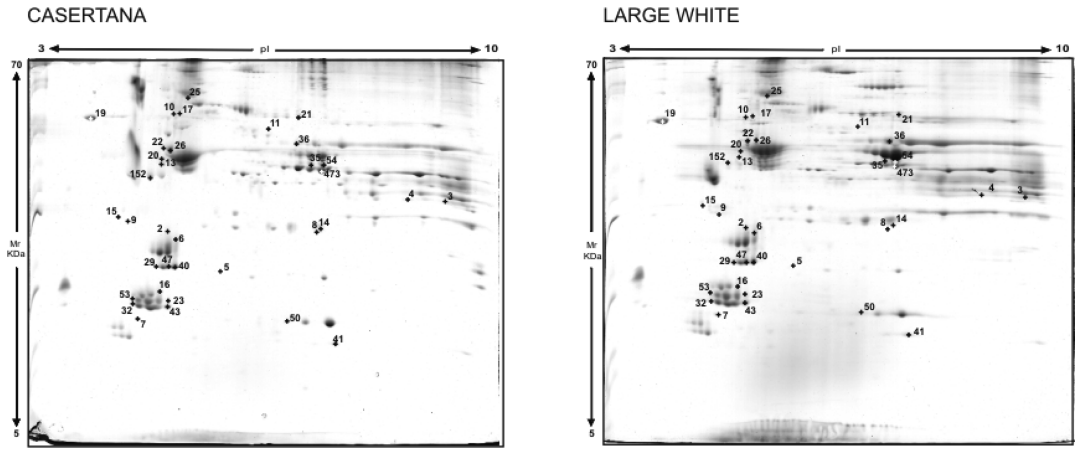

Figure 1. 2-DE of *longissimus lumborum* extracts from Large White and Casertana pig breeds. IEF pH range is 3−10, 12% T 3% C Acrylamide. Gels have been stained with Colloidal Coomassie. Each gel image has been elaborated with Progenesis SameSpots (Nonlinear Dynamics, NewCastle, U.K.) and represent an average of 30 gels (3 technical replicate for 10 biological replicate samples), upon background subtraction.

Promega, Madison, WI) in an ice bath. After 30 min, the supernatant was removed and discarded; then 20 mL of 50 mM NH_4HCO_3 were added to the gel pieces, and digestion was allowed to proceed overnight at 37 °C. The supernatant containing tryptic peptides was dried by vacuum centrifugation. Prior to mass spectrometric analysis, the peptide mixtures were redissolved in 10 μL of 5% FA (formic acid).

Protein Identification by Nano-RP-HPLC−ESI−MS/MS. Mass spectrometric procedures were performed as previously described.[22] Peptide mixtures were separated using nanoflow-HPLC system (Ultimate; Switchos; Famos; LC Packings, Amsterdam, The Netherlands). A sample volume of 10 μL was loaded by the autosampler onto a homemade 2 cm fused silica precolumn (75 μm I.D.; 375 μm O.D) Reprosil C18-AQ, 3 μm (Ammerbuch-Entringen, DE) at a flow rate of 2 μL/min. Sequential elution of peptides was accomplished using a flow rate of 200 nL/min and a linear gradient from Solution A (2% acetonitrile; 0.1% formic acid) to 50% of Solution B (98% acetonitrile; 0.1% formic acid) in 40 min over the precolumn in-line with a homemade 10−15 cm resolving column (75 μm I.D.; 375 μm O.D.; Reprosil C18-AQ, 3 μm (Dr. Maisch GmbH, Ammerbuch-Entringen, Germany). Peptides were eluted directly into a High Capacity ion Trap HCTplus (Bruker-Daltonik, Bremen, Germany). Capillary voltage of 1.5−2 kV and a dry gas flow rate of 10 L/min were used at a temperature of 200 °C. The scan range used was from 300 to 1800 m/z. Protein identification was performed by searching in the National Center for Biotechnology Information nonredundant database (NCBInr, version 20081128, www.ncbi.nlm.nih.gov) using the Mascot program in-house version 2.2 (Matrix Science, London, U.K.). The following parameters were adopted for database searches: complete carbamidomethylation of cysteines and partial oxidation of methionines, peptide Mass Tolerance ±1.2 Da, Fragment Mass Tolerance ±0.9 Da, missed cleavages 2. For positive identification, the score of the result of $(-10 \times \mathrm{Log}(P))$ had to be over the significance threshold level ($P < 0.05$). Even though high MASCOT scores are obtained with values greater than 60, when proteins were identified by one peptide only a combination of automated database search and manual interpretation of peptide fragmentation spectra was used to validate protein assignments. In this manual verification the mass error, the presence of fragment ion series and the expected prevalence of C-terminus containing ions (Y-type) in the high mass range were all taken into account. Moreover, replicate measurements have confirmed the identity of the protein hits.

Phosphorylated Proteins Identification. Gels have been washed three times with double distilled water and then stained with ProQ diamond (Invitrogen, Carlsbad, CA) for 2 h, following manufacturer's instructions. Stained gels have been washed three times with a 100 mM Sodium Acetate, 20% Acetonitrile solution for destaining. Images have been acquired with a *Gel Doc* XR System (Biorad), through UV-ray fluorescence and matched against coomassie stained gels.

RNA Sample Extraction. Longissimus lumborum muscle samples of LW and CA individuals (see above) were collected immediately after slaughtering. Samples were preserved in RNA later (Sigma-Aldrich) and stored at −80 °C. Total RNA was extracted by using TRIzol Plus RNA purification kit (Invitrogen). RNA integrity was assessed by electrophoretic analysis of 28S and 18S rRNA subunits. RNA purity and concentration were assessed with the spectrophotometer GeneQuant*pro* (Amersham Pharmacia Biotech, Uppsala, Sweden); A260/A280 ratio was >1.9. Besides RNA concentration was measured by using the Quant-iT RNA Assay kit (Molecular Probes) on the DTX 880 fluorometer (Beckman Coulter, Brea, CA).

Microarray Experiments. RNA samples from the 10 animals of each breed were pooled as to reduce the total amount of needed material and because the primary interest was to put evidence on breed-specific gene expression changes rather than individuals.[23,24]

An amount of 1 μg of pooled RNA was first reverse transcripted and then amplified by using the RNA ampULSe kit (Kreatech, Amsterdam, The Netherlands) following manufacturer's instructions. Four μg of aRNA for each pool were labeled with Cy3 and Cy5 dye independently; for the repeat slide the same comparison was made with the dye assignment reversed (dyeswap).[25] A technical replicate was performed starting from the same RNA pool (4 slides). A biological replicate of the previous experiment was obtained starting with independent RNA preparation from the same sample tissues (4 slides).[26] The slides were spotted by CRIBI service with the 70mer Pig Genome Oligo Set Version 1.0 (Operon) representing the 10 665 *Sus scrofa* gene sequences replicated twice. Annotations for oligo sequences were update on March 2006. The hybridizations were performed at 48 °C for 18 h by using the HybChamber (GeneMachines, San Carlos, CA).

Microarray Data Analysis. Hybridization images were scanned with the Packard ScanArray Express Line of Microarray Scanners (PerkinElmer Life Sciences, Waltham, Massachussets). Spotfinder software (TIGR) was used to extract feature data from microarray fluorescence images. Slides were first preprocessed filtering spots with poor hybridization signals, saturated signals, or signal to background ratio lower than two. Then lowess and dye-swap normalizations were applied.[27]

To establish the significance of observed regulation for each gene, *t* test with Welsh's correction was performed. Finally, only genes with Fold-Change over |1.3| were considered (Benjamini/−/Hochberg adjusted $P < 0.05$).

Network Analyses. Preliminary network analyses were performed as previously reported.[28,29] Two original lists of proteins and gene transcripts were obtained from proteomics and transcriptomics differential analyses. The lists (either merged or alone) were submitted for elaboration of network analyses to the Ingenuity Pathway Analysis (IPA) software (Ingenuity Systems,www.ingenuity.com).[30] Each gene identifier from the submitted list was mapped to its corresponding gene object in the Ingenuity Pathways Knowledge Base. The significance of the association between the data set and the canonical network was measured in 2 ways:

(1) A ratio of the number of proteins from the data set that map to the pathway divided by the total number of proteins that map to the canonical pathway is displayed.

(2) Fischer's exact test was used to calculate a *p*-value determining the probability that the association between the proteins in the data set and the canonical pathway is explained by chance alone.

Highest scores are proportional to a lower probability of casual association. The IPA software allowed us to perform an unbiased elaboration of the available data, in order to focus subsequent analyses and discussions on the pivotal networks.

Network analysis delves into protein−protein interactions and exploits them to give an intuitive portrait of the relationships among pivotal molecules and, on a higher level, among networks. The software determines and graphs unbiased networks, in which gene products are represented as nodes, and the biological relationship between two nodes is represented as an edge (line). All edges are supported by at least 1 reference from the literature, from a textbook, or from canonical information stored in the Ingenuity Pathways Knowledge Base. Nodes are displayed using various shapes that represent the functional class of the gene product. Gray nodes represent the proteins from the submitted data set which have a match in the canonical pathway from the database, while white nodes represent gene products that the software attributed to the same networks, although they were not present in the elaborated data set. Continuous lines (edges) represent direct interactions, while indirect ones are represented by interrupted lines. Circular lines around one node describe a feed-back loop of activity of that node on itself (e.g., by self-modulating its activity or expression). Gray edges represent interactions within a single network (intranetwork), while orange edges cross-link nodes from multiple interacting networks (cross-network).

In a general point of view, IPA software was initially developed for the study of pathologies and mainly focused on cancer. As a consequence, many of the retrieved pathways are related to diseases, in particular to cancer. Clearly, this software is not well adapted for the study of pig proteins. To fix this difficulty, IPA or equivalent software should first be used to establish some group of proteins. Therefore, proteomics data were also elaborated for network analysis with Cytoscape,[31] exploiting the APID2NET plugin.[32] Data were treated as to include all the proteins individuated upon the experimental phase, including isoforms and excluding redundant entries. The software interrogates freely available online database for interactomics analysis, namely BioGrid (version 2.0.47), BIND (version 04−05−06), DIP (version 14−10−08), HPRD (version 7), IntAct (version 2008−12−12), MINT (version 2008−10−23). Interaction data are compared against standard proteomics databases for protein identification through IDs, names and descriptions, such as UniProt, and validated with iPfam (for domain−domain interaction-pattern recognition. Cut-off values were set as to include in the protein−protein interaction analyses only those nodes which have been reported as interactors in at least 3 experimental publications and with at least two different techniques. Experimentally individuated proteins are represented as red nodes, while white nodes represent those proteins which the software has individuated as likely interactors through stringent analysis.

This multiplatform network analysis guarantees that the individuated networks were not biased by the software, while clearly elucidating the topology of the protein−protein interaction maps and their actual biological implications.

Functional Enrichment of GO Terms. In a second approach, some of the representing proteins should be examined in databases to get additional annotations on their functions and consequently to establish some hypothesis concerning their functions in the suckling upon lactation.

FatiGO/Babelomics[33−35] takes one list of genes and compares it against the rest of the human genome upon conversion of the protein entries into a list of GO terms, using the corresponding gene-GO association table. Then a Fisher's exact test is used to check for significant over-representation of GO terms in the submitted data set against the rest of the genome.

Results and Discussions

In the present study, we investigated protein composition of *longissimus lumborum* muscle samples from LW and CA pig breeds. In parallel, samples were also analyzed with transcriptomics techniques.

Proteomics analyses (2-DE and MS/MS identification) yielded a total of 473 ± 44 spots which were commonly expressed by both breeds, and 36 differentially expressed spots ($P \leq 0.05$) upon comparison of 60 gels (30 per breed, 10 biological replicates and 3 technical replicates each). In particular, 13 spots were up-regulated in CA and 20 in LW. Approximately 95% of these spots were identified via ESI−MS/MS. In Table 1 the identities are listed of the successfully identified proteins, together with the standard spot number, the identification parameters, and the indication of their gene ontology (GO) annotation (molecular function).

Notably, mass spectrometric identification of those spots revealed that most of those spots accounted for the same protein (mainly glycolytic enzymes in CA and myosin light chain isoforms in LW, see also Table 1), as to yield a total of 9 different up-regulated proteins in CA and 10 counterpart entries for LW (Table 1). Some proteins have multiple duplicate entries in the table, such as creatine kinase M chain for CA (3 entries) and myosin light chain 1f in LW (4 entries).

For example, spots 29 and 47 from LW, accounting for the same protein (myosin light chain 1f), displayed a similar quantitative trend. Analogous observations could be made for spots 21, 473, and 54 (creatine kinase M-type), which are

Table 1. Differential Proteomics Analysis[a]

N spot[b]	M_r, kDa theor/exp[c]	p*I* theor/exp[c]	no. of peptides identified	Mascot score	NCBI accession number	protein ID [Sus scrofa]
			Casertana			
CAspot3	36.9/32.0	8.2/9.2	9	460	gi|1170740	L-lactate dehydrogenase A chain (LDH-A) (LDH muscle subunit) (LDH-M) [Sus scrofa]
CAspot4	36.9/32.0	8.2/8.7	6	388	gi|1170740	L-lactate dehydrogenase A chain (LDH-A) (LDH muscle subunit) (LDH-M) [Sus scrofa]
CAspot7	15.1/17.0	4.9/4.7	5	463	gi|3746944	phosphoglucomutase 1 [Sus scrofa]
CAspot8	22.1/25.8	6.0/7.3	12	655	gi|91214448	triosephosphate isomerase 1 [Sus scrofa]
CAspot11	54.1/54.0	6.0/6.6	5	266	gi|119917044	Similar to tripartite motif-containing 72 [*Homo sapiens*]
CAspot14	22.1/25.8	6.0/7.4	17	973	gi|91214448	triosephosphate isomerase 1 [Sus scrofa]
CAspot15	20.3/29.0	5.0/4.7	8	380	gi|2149959	cytosolic glycerol-3-phosphate dehydrogenase [Sus scrofa]
CAspot 21	43.3/54.7	6.6/7.3	20	1021	gi|62286641	Creatine kinase M-type (Creatine kinase M chain) [Sus scrofa]
CAspot35	47.4/40.5	8.0/7.3	19	1079	gi|113205498	enolase 3 [Sus scrofa]
CAspot36	44.8/44.0	8.0/7.0	10	564	gi|47169448	Chain A, Structure Of Pig Muscle Pgk Complexed With Mgatp [Sus scrofa]
CAspot50	17.1/17.1	6.8/7.0	2	72	gi|230253	Chain A, The Determination Of The Crystal Structure Of Recombinant Pig Myoglobin By Molecular Replacement And Its Refinement [Sus scrofa]
CAspot54	43.3/40.5	6.6/7.4	15	866	gi|62286641	Creatine kinase M-type (Creatine kinase M chain) [Sus scrofa]
CAspot473	43.3/39.0	6.6/7.4	14	843	gi|62286641	Creatine kinase M-type (Creatine kinase M chain) [Sus scrofa]
			Large White			
LWspot2	21.0/26.1	4.9/5.2	13	782	gi|117660874	MLC1f [Sus scrofa]
Lwspot5	22.9/23.1	5.8/5.7	4	217	gi|9968807	alpha-1-antichymotrypsin 3 [Sus scrofa]
LWspot6	21.0/26.1	4.9/5.3	12	824	gi|117660874	MLC1f [Sus scrofa]
LWspot9	26.4/29.0	4.8/4.7	5	268	gi|530049	14-3-3 protein [Ovis aries]
LWspot10	42.2	5.3/5.2	4	210	gi|6653228	skeletal alpha-actin [Sparus aurata]
LWspot13	30.3/41.0	5.4	13	638	gi|164359	apolipoprotein A-I [Sus scrofa]
LWspot16	19.1/20.5	4.9/5.1	16	884	gi|54607195	myosin regulatory light chain 2 [Sus scrofa]
LWspot17	42.2/55.2	5.2/5.2	4	239	gi|30268609	skeletal alpha-actin type-2b [Coryphaenoides yaquinae]
LWspot19	44.9/55.0	4.0/3.8	2	109	gi|118150866	calsequestrin 1 [*Bos taurus*]
LWspot20	42.4/41.5	5.3/5.2	7	578	gi|27819614	actin, alpha 1, skeletal muscle [*Bos taurus*]
LWspot22	45.7/44.1	5.8/5.3	4	218	gi|61553131	alpha 2 actin [*Bos taurus*]
LWspot23	19.1/19.0	4.9/5.2	5	353	gi|54607195	myosin regulatory light chain 2 [Sus scrofa]
LWspot25	NI	–	–	–	–	–
LWspot26	42.3/44.2	5.2/5.4	9	663	gi|268607671	actin, alpha skeletal muscle [Sus scrofa]
LWspot29	21.0/23.4	4.9/5.0	14	868	gi|117660874	MLC1f [Sus scrofa]
LWspot32	19.1/18.0	4.9/4.7	12	767	gi|54607195	myosin regulatory light chain 2 [Sus scrofa]
LWspot40	14.3/23.4	4.7/5.3	3	128	gi|1717797	Peroxiredoxin-2 (Thioredoxin peroxidase 1) (Thioredoxin-dependent peroxide reductase 1) (Thiol-specific antioxidant protein) (TSA) [Sus scrofa]
Lwspot41	16.1/14.0	6.8/7.4	11	886	gi|809283	Chain B, Structure Determination Of Aquomet Porcine Hemoglobin At 2.8 Angstrom Resolution
LWspot43	19.1/18.0	4.9/5.2	12	929	gi|54607195	myosin regulatory light chain 2 [Sus scrofa]
LWspot47	21.0/23.4	4.9/5.2	13	803	gi|117660874	MLC1f [Sus scrofa]
LWspot53	16.7/19.0	4.6/4.7	5	244	gi|127135	Myosin light chain 3, skeletal muscle isoform (A2 catalytic) (Alkali myosin light chain 3) (MLC3F) [Oryctolagus cuniculus]
LWspot152	NI	–	–	–	–	–

[a] Protien differentially expressed fro Large White and Casertana pig breeds were Identified on the basis of Figure 1. [b] Spot number represents the number on the master gel (see Figure 1). [c] Theoretical M_r/p*I* was calculated with M_r/p*I* tool on the Expasy Web site (http://expasy.org/tools/pi_tool.html).

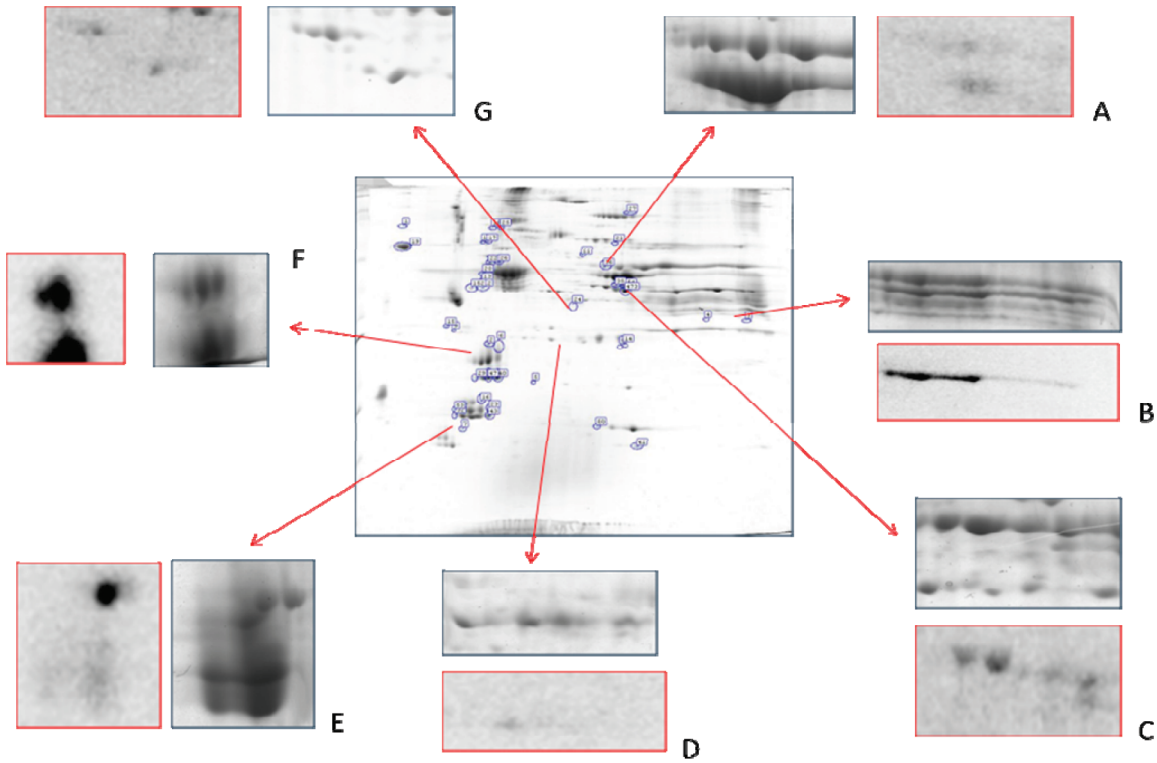

Figure 2. Phosphorylated proteins recognized by ProQ-Diamond staining are shown. (A) Enolase; (B) Lactate Dehydrogenase; (C) Creatine Kinase; (D) NI; (E) Myosin Regulatory Light Chain 2; (F) Myosin Light Chain 1, Fast; (G) cytosolic glycerol-3-phosphate dehydrogenase. Coomassie staining is shown squared in blue, corresponding ProQ Diamond staining squared in red.

reported in Figure 1. These observations could suggest that breed-specific characteristic probably rely on further differential post-translational modifications of pivotal enzymes, other than on their specific differential expression. However, ProQ diamond staining for the characterization of the phosphorylation pattern through specific staining of 2D gels confirmed that most of these duplicate entries showing only slight differences in pH were represented by differently phosphorylated proteins (Figure 2 for details).

Microarray analyses have individuated a total of 105 differentially expressed gene transcripts with a fold change > 1.3 (Table 2). In detail, 66 gene transcripts were up-regulated in CA and 39 in LW pigs. Little or no direct overlap between transcriptomics and proteomics data was observed, as previously reported.[36,37] These differences may arise from annotation errors or differential regulation of translation, turnover or alternative splicing.[36] However, in addition to various biological factors, it should be considered that the poor correlation between transcriptomic and proteomic data could be quite possibly due to the inadequacy of available statistical tools to compensate for biases in the data collection methodologies as well as to the different bioinformatic approaches employed to analyze and integrate data from either proteomics or genomics studies.[38] There are also difficulties in evaluating on a global level which biological factor, translational efficiency or protein half-life, influences the correlation between mRNA and protein abundances to time-course differences between mRNA changes and protein responses.[4,39]

It has been previously observed[29] that, although proteomics and transcriptomics experimental data sets display low to absent overlap, interaction pathway analyses allow the individuation of central networks sharing the same biological meaning.

Under this perspective, proteins and gene transcripts indirectly converged in CA, as they mainly belonged to metabolic pathways - glycolytic and glycolysis-related enzymes, such as Enolase 3 (ENO3), Triosephosphate Isomerase (TPI), Phosphoglucomutase1 (PGM1), Lactate Dehydrogenase (LDHA), Glucose 3-Phosphate Dehydrogenase (GPDH) and Creatine Kinase (CK-M) in Table 1; Ketoexokinase (KHK) in Table 2)—enzymes involved in (i) fatty-acid oxidation responses—glutaredoxin 3 (GRX3), thioredoxin 2 TRX2; (ii) calcium homeostasis - S100 calcium binding protein A2 (S100A2), (iii) hormone inducers/growth factors/regulators of transcription (hydroxy-delta-5-steroid dehydrogenase (HSD3B2), NFKB inhibitor interacting Ras-like 1 (NKIRAS1), bromodomain containing 4 (BRD4), leucine-rich repeat kinase 1 (Lrrk1), silent mating type information regulation 2 homologue 2 (SIRT1).

Conversely, proteins and gene transcripts which were found to be overexpressed in LW *longissimus* muscle mainly accounted for (i) structural muscle proteins—myosin light chain (MLC) isoforms 1f, 2, 2 V and 3; alpha-actin (ACTA1); (ii) proteins involved in the maintenance of the balance between protein synthesis and degradation - E3 ubiquitin-protein ligase (MARCH5), ring finger protein 128 (RNF128), SERPINA3; (iii) fatty-acid oxidation and oxidative stress response—carnitine palmitoyltransferase 1C (CPT1), Glutathione peroxidase 5 (GPRX5), Peroxiredoxin-2 (PRX2); (iv) transcription regulators—retinoic acid receptor alpha (RARA), estrogen related receptor alpha (ESRRA), basic leucine zipper and W2 domain-containing protein 2 (BZW2), zinc finger protein 212 (ZNF212).

These preliminary observations were confirmed upon GO term enrichment of biological function in CA *Longissimus* up-regulated proteins and transcripts (Table 3, left side). Indeed, CA muscles appeared to be particularly enriched in GO terms involving glycolytic catabolism (catabolic process, cellular

Table 2. Differentially-Expressed mRNAs from Microarray Screening of Casertana and Large White Transcripts in *longissimus* Muscle[a]

N.	gene Id	Unigene Sus	gene	gene encoding	fold change	*p*-value
			Large White			
1.	gi|194044553	Ssc.49967	NP_115590.1	Similar to Srclikeadaptor 2 isoform a	1.30215	0.001452
2.	gi|194034423	Ssc.48760	L2HGDH	Similar to L-2-hydroxyglutarate dehydrogenase precursor	1.30235	0.000268
3.	gi|194040450	Ssc.1094	GLO1	Similar to glyoxalase I	1.30615	0.002367
4.	gi|190360625	Ssc.8984	ARHGEF2	rho/rac guanine nucleotide exchange factor (GEF) 2	1.30895	0.012928
5.	gi|22748777	Ssc.18511	CPT1C	Strongly similar to carnitine palmitoyltransferase 1C isoform 2	1,3153	0.013585
6.	gi|219522004	Ssc.54776	MAPKAPK3	Mitogen-activated protein kinase activated-protein kinase 3	1,32111	0,028946
7.	gi|37588873	Ssc.18929	RNF128	ring finger protein 128	1,32246	0,022308
8.	gi|194035579	Ssc.5132	FAM84B	family with sequence similarity 84, member B	1,32584	0,00897
9.	gi|51873031	Ssc.11130	NCLN	strongly similar to nicalin precursor [*Homo sapiens*]	1,3287	0,004981
10.	gi|237681314	Ssc.3153	NP_001020461.1	developmental pluripotency associated 5	1,33176	0,018456
11.	gi|10092639	Ssc.18546	LOC100070329	similar to cysteine-rich motor neuron 1 protein precursor [*Homo sapiens*]	1,34622	0,001207
12.	gi|194037340	Ssc.15828	RARA	Retinoic acid receptor, alpha	1,34798	0,000997
13.	gi|31083243	Ssc.6731	PPP2R5C	protein phosphatase 2, regulatory subunit B', gamma isoform	1,34823	0,021911
14.	gi|24797065		ZNF212	zinc finger protein 212	1,35108	0,036852
15.	gi|1469874	Ssc.61966	LOC100050625	similar to Uncharacterized protein KIAA0146	1,3546	0,033324
16.	gi|149193321	Ssc.12808	GRSF1	Grich RNA sequence binding factor 1	1,35556	0,002732
17.	gi|13938355	Ssc.7378	ATP6 V1B2	ATPase, H+ transporting, lysosomal 56/58 kDa, V1 subunit B2	1,35894	0,00147
18.	gi|8923900	Ssc.1763	CMAS	cytidine monophosphate Nacetylneuraminic acid synthetase	1,37176	0,000527
19.	gi|220732380		FREM1	FRAS1 related extracellular matrix 1	1,37538	0,010872
20.	gi|29788758	Ssc.39944	LOC652955	similar to goliath Homologue precursor [*Homo sapiens*]	1,37623	0,012116
21.	gi|55859666	Ssc.18510	XP_001493829.1	Similar to actin binding LIM protein 1 [*Homo sapiens*]	1,37654	0,046034
22.	gi|148763347	Ssc.70866	XP_001713795.1 replaced in database by NP_076916	similar to cell division protein kinase 11A isoform 1 [*Homo sapiens*]	1,37909	0,048123
23.	gi|209915561	Ssc.60309	LOC506315	similar to dynamin 3 [*Homo sapiens*]	1,37985	0,012045
24.	gi|239049447	Ssc.6166	LOC100061008	similar to malic enzyme 3, NADP(+)dependent, mitochondrial precursor [*Homo sapiens*]	1,38554	0,010694
25.	gi|171465894	Ssc.2330	SLC3A2	Solute carrier family 3 (activators of dibasic and neutral amino acid transport), member 2	1,40501	0,005402
26.	gi|33636756	Ssc.40278	MARK4	Similar to MAP/microtubule affinity regulating kinase 4	1,40557	0,049369
27.	gi|209977023	Ssc.15262	LOC100068640	moderately similar to NP_872425.2 secretory protein LOC348174 precursor [*Homo sapiens*]	1,40972	0,036035
28.	gi|47523090	Ssc.14513	GPX5	Glutathione peroxidase 5 (epididymal androgenrelated protein)	1,41346	0,015261
29.	gi|168229161	Ssc.60909	CORO7	Similar to coronin 7 (*Homo sapiens*)	1,4171	0,011396
30.	gi|18860920	Ssc.55256	Esrra	strongly similar to NP_004442.3 estrogen-related receptor alpha [*Homo sapiens*]	1,43313	0,017213
31.	gi|21389315	Ssc.17264	SLC25A1	Similar to solute carrier family 25 (mitochondrial carrier; citrate transporter), member 1[*Homo sapiens*]	1,43735	0,010343
32.	gi|229577398	Ssc.51869	LOC100053031	similar to Basic leucine zipper and W2 domaincontaining protein 2	1,44724	0,017316
33.	gi|119570479	Ssc.7478	LOC788125	similar to E3 ubiquitinprotein ligase MARCH5 (Membraneassociated RING finger protein 5) (Membraneassociated RINGCH protein V) (MARCHV) (RING finger protein 153)	1,45647	0,044993
34.	gi|6634023	Ssc.29073	LOC531863	similar to Pleckstrin Homology domaincontaining family M member 1 (162 kDa adapter protein) (AP162)	1,45783	0,003205

Table 2. Continued

N.	gene Id	Unigene Sus	gene	gene encoding	fold change	*p*-value
35.	gi|89353283	Ssc.6230	SDCCAG3	Moderately similar to serologically defined colon cancer antigen 3	1,46199	0,000443
36.	gi|189083684	Ssc.6514	Gale	Strongly similar to galactose4 epimerase, UDP	1,49271	0,000377
37.	gi|144922657	Ssc.6826	SELK	Selenoprotein K	1,51373	0,020642
38.	gi|113205850	Ssc.57041	RGS2	regulator of G protein signaling 2, 24 kDa	1,51615	0,017288
39.	gi|194038117	Ssc.49381	4930573I19Rik	RIKEN cDNA 4930573I19 gene	1,54825	0,019928
				Casertana		
1.	gi|34577087	Ssc.2212	RNF13	ring finger protein 13	1,93087	0,011911
2.	gi|62420888	Ssc.49801	LOC100059924	similar to Dipeptidylpeptidase 7	1,91137	0,014412
3.	gi|194036051	Ssc.54527	LOC719341	similar to LOC526125 protein (Dingo protein isoform 1)	1,80105	0,000741
4.	gi|5902134	Ssc.13176	Coro1a	coronin, actin binding protein 1A	1,76507	0,009432
5.	gi|194035490	Ssc.50346	LOC100064627	hypothetical protein LOC100064627 similar to RecQ protein-like 4 isoform 1	1,69498	0,002568
6.		Ssc.14202		Transcribed locus	1,64555	0,003126
7.	gi|194038510	Ssc.5780	LOC100054565	similar to pecanex-like protein 1	1,61993	0,001504
8.	gi|18390344	Ssc.19644	ATRIP	ATR interacting protein	1,61518	0,004452
9.	gi|19923621	Ssc.11534	NP_079469.2	Hydroxy-delta-5-steroid dehydrogenase, 3 beta and steroid deltaisomerase 7	1,61352	0,033153
10.	gi|47523440	Ssc.57585	SLC23A2	Solute carrier family 23 (nucleobase transporters), member 2	1,57817	0,009305
11.	gi|256773260	Ssc.54720	TIMM8B	mitochondrial import inner membrane translocase subunit Tim8 B	1,55179	0,004532
12.	gi|194034004	Ssc.18454	TLE1	Similar to transducin-like enhancer protein 1 (LOC100157241)	1,5299	0,004166
13.		Ssc.54014		Transcribed locus	1,52761	0,03567
14.	gi|55741443	Ssc.70373	PAG6	Similar to pregnancy-associated glycoprotein 6	1,52585	0,001232
15.	gi|255759955	Ssc.21896	LOC100072409	Similar to WD repeat domain 81 isoform 4	1,5155	0,012373
16.	gi|22547159	Ssc.11419	LOC100073148	similar to tetratricopeptide repeat domain 19	1,50752	0,023896
17.	gi|194044705	Ssc.12924	NCOA5	Similar to nuclear receptor coactivator 5	1,49957	0,000886
18.	gi|256838109	Ssc.70871 (retired) New: Ssc.42571	LOC608816	Similar to solute carrier family 25 (mitochondrial carrier; phosphate carrier), member 3	1,49845	0,015786
19.	gi|178056229	Ssc.55376	RBM4	RNA binding protein 4	1,49104	0,035514
20.	gi|9966809	Ssc.12641	NKIRAS1	Similar to kappa B-ras 1	1,48267	0,001218
21.	gi|4506967	Ssc.27983	CSKI	Similar to v-ski sarcoma viral oncogene Homologue	1,48264	0,001322
22.	gi|156120132	Ssc.54918	NR1H3	Nuclear receptor subfamily 1, group H, member 3	1,47355	0,003882
23.	gi|4503563	Ssc.11016	LOC717867	similar to Epithelial membrane protein 3	1,46876	0,012115
24.	???	Ssc.2047	FNDC3A	fibronectin type III domain containing 3A	1,46643	0,02612
25.	gi|55741813	Ssc.211	TRAINA	Putative pancreatic ribonuclease precursor	1,45406	0,012041
26.		Ssc.35609		Transcribed locus	1,45282	0,006403
27.	gi|148231223	Ssc.49478	MAVS	Mitochondrial antiviral signaling protein	1,44677	0,010636
28.	gi|133922600	Ssc.59509	SFRS16	splicing factor, arginine/serinerich 16	1,44532	0,014511
29.		Ssc.54615		Transcribed locus	1,44353	0,040486
30.	gi|33695078		LOC709587	similar to protein phosphatase 2, regulatory subunit B, beta isoform 1	1,44178	0,024297
31.	gi|194043140	Ssc.25105	CRYBB3	similar to beta-B3 Crystallin	1,44117	0,038394
32.	gi|166796035	Ssc.6381	SIRT2	Sirtuin (silent mating type information regulation 2 Homologue) 2	1,43879	0,042071
33.	gi|15147240	Ssc.24837	BOC	strongly similar to NP_150279.1 brother of CDO precursor	1,43443	0,000755
34.	gi|47523436	Ssc.16086	OPRL	Orphanin FQ/nociceptin receptor	1,42946	0,017954
35.	gi|298104080	Ssc.60025	RAB11FIP4	similar to ribosomal protein L30 isoform 2	1,42871	0,044632
36.	gi|80971504	Ssc.55003	NPAL3	ribosomal protein SA	1,4263	0,014475
37.	gi|115430241	Ssc.9051	LTBP3	similar to SCY1-like 1 isoform A	1,41497	0,002041
38.	gi|194042067	Ssc.18510		similar to actin binding LIM protein 1	1,4131	0,040943
	gi|145701012		LOC703083	similar to EGL nine (C.elegans) Homologue 2	1,41288	0,000814

Table 2. Continued

N.	gene Id	Unigene Sus	gene	gene encoding	fold change	*p*-value
39.	gil156416005	Ssc.2256	COMMD9	COMM domain containing 9	1,41273	0,028578
40.	gil5670342	Ssc.5996	KHK	ketohexokinase (fructokinase)	1,40936	0,02108
41.	gil28416946	Ssc.54531	LOC519634	myosin-XVIIIa isoform a	1,40696	0,02938
	gil66347768		LOC612166	similar to Absent in melanoma 1 protein	1,39789	0,013524
42.	gil47522674	Ssc.14550		matrix metalloproteinase 25 precursor	1,39241	0,010134
43.	gil21361403	Ssc.14827	LOC100069490	similar to thioredoxin 2 precursor	1,38949	0,033595
44.	gil194035143	Ssc.55109		Similar to Uncharacterized protein C6orf203 (LOC100157575)	1,38203	0,025584
45.	gil90991702	Ssc.25233	LRRK1	leucine-rich repeat serine/ threonine-protein kinase 1	1,37715	0,001965
46.	gil46575934	Ssc.28748	LOC616908	KIAA1680 protein isoform 2	1,37613	0,029454
47.	gil17149842	Ssc.54360	FKBP2	FK506 binding protein 2, 13 kDa precursor	1,37603	0,014657
48.	gil7661622	Ssc.68154	LOC782016	hypothetical protein LOC25906 [*Homo sapiens*]	1,37502	0,010824
49.	gil157671951	Ssc.44921	SLC4A3	solute carrier family 4, anion exchanger, member 3	1,37466	0,02771
50.	gil34335194	Ssc.58414	LOC100018119	cAMP responsive element modulator isoform g	1,36276	0,025195
51.	gil239835767	Ssc.48672	LOC100071758	similar to Developmental pluripotency associated 2	1,35267	0,014497
52.	gil194040419	Ssc.7179	LOC618886	similar to Uncharacterized protein C6orf89 Homologue	1,35163	0,000348
53.	gil194036153	Ssc.12269	S100A2	similar to Protein S100-A2 (S100 calcium-binding protein A2) (Protein S-100 L) isoform 2	1,34902	0,011624
54.	gil7657218	Ssc.28006	BRD4	bromodomain-containing protein 4 isoform short	1,34479	0,019024
55.	gil187607085		LOC100054101	similar to E3 ubiquitin-protein ligase LNX isoform a	1,33575	0,027296
56.	gil110815802	Ssc.60174	LOC709210	hypothetical protein LOC84267	1,33436	0,003368
57.	gil50979297	Ssc.5575	ELS1	Pancreatic elastase I precursor	1,33051	0,019014
58.	gil171460918	Ssc.24428	DNM1L	dynamin 1-like isoform 3	1,32822	0,00286
59.	gil224809399	Ssc.50353	LOC511316	Strongly similar to hypothetical protein LOC729991 isoform 1	1,31815	0,028298
60.	gil144226847	Ssc.48643	OBSL1	obscurin-like 1	1,31806	0,00608
61.	gil194272180	Ssc.40232	PLXNB1	Similar to plexin B1 precursor	1,30931	0,020747
62.	gil47522778	Ssc.5053	CD163	CD163 antigen	1,30663	0,03586
63.	gil95113651	Ssc.20426	NP_006532.2	strongly similar to glutaredoxin 3	1,30587	0,0136
64.	gil29826282	Ssc.54826	LOC100055191	strongly similar to protein phosphatase 1G	1,30433	0,006456

[a] Proteins predicted from Ssc sequences have been found using Unigene database (NCBI) and listed with corresponding gi identifiers. Where possible, proteins from Sus scrofa have been chosen, otherwise the closest proteins from Homo sapiens have been added.

Table 3. GO Term Enrichment in Large White and Casertana Pigs

GO term	
Casertana	Large White
catabolic process (GO:0009056)	muscle contraction (GO:0006936)
vitamin metabolic process (GO:0006766)	response to stress (GO:0006950)
cellular catabolic process (GO:0044248)	developmental maturation (GO:0021700)
glycerol metabolic process (GO:0006071)	lipid metabolic process (GO:0006629)
L-ascorbic acid metabolic process (GO:0019852)	oxygen and reactive oxygen species metabolic process (GO:0006800)
glycerol-3-phosphate metabolic process (GO:0006072)	regulation of lipid metabolic process (GO:0019216)
tricarboxylic acid cycle intermediate metabolic process (GO:0006100)	regulation of cell proliferation (GO:0042127)
cellular carbohydrate catabolic process (GO:0044275)	muscle development (GO:0007517)
hexose metabolic process (GO:0019318)	oxidative phosphorylation (GO:0006119)

catabolic process, glycerol metabolic process, glycerol-3-phosphate metabolic process, cellular carbohydrate catabolic process, hexose metabolic process) and vitamin metabolism (vitamin metabolic process, L-ascorbic acid metabolic process).

Biological function analyses confirmed the role of (i) muscle growth (developmental maturation, regulation of cell proliferation, muscle development) and contraction/response to stress (muscle contraction, response to stress); (ii) lipid metabolism (lipid metabolic process, regulation of lipid metabolic process); and, adding a further detail, (iii) oxidative metabolism (oxygen and reactive oxygen species metabolic process, oxidative phosphorylation; Table 3). Whether a molecular correlation between

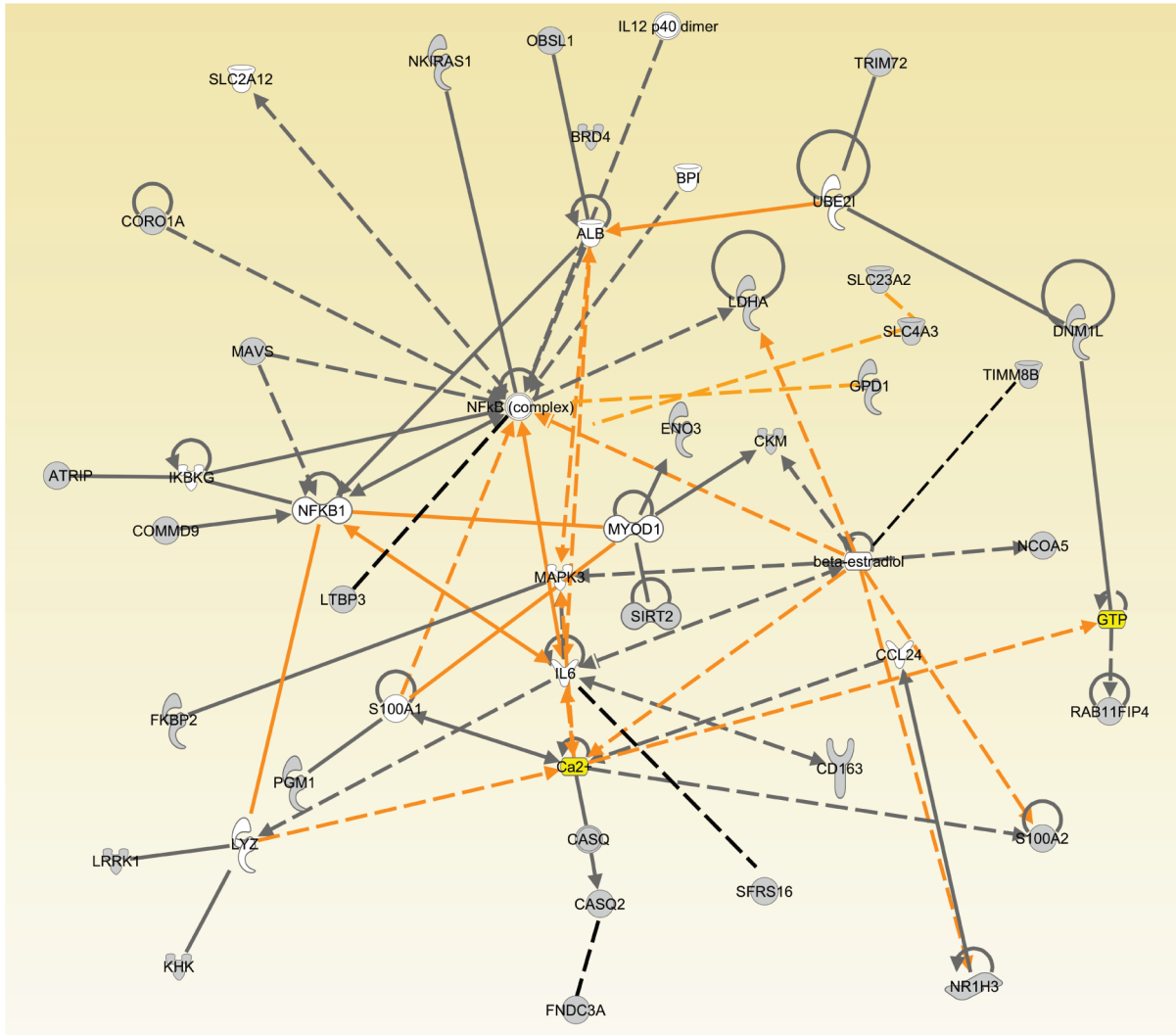

Figure 3. Top network from network analysis via Ingenuity Pathway Analysis in Casertana merged protein and microarray data. Gray nodes: proteins from the data set having a match in the databas. White nodes: proteins from the database which were not identified (if present) upon the experimental phase. Yellow nodes: nonprotein molecules. Gray edges: interactions within a network. Continuous line - edge: direct interaction. Interrupted line - edge: indirect interaction.

predisposition to adipogenesis and molecular profiles surely exists, it is more likely distributed on wide networks of proteins instead of relying on single specific molecules. This is the reason why we focused on protein−protein interaction networks of the individuated data sets. A multiplatform network analysis was performed with IPA for CA (Figure 3) and LW (Figure 4) and Cytoscape/APID2NET (Figure 5), as the former provides clearly interpretable top score networks, at the expenses of the clarity of the whole merged interactome, while the latter gives the opportunity to customize a series of criteria in order to produce a more or less stringent analysis. Another relevant issue of the Ingenuity software is its bias toward human hortologues of swine proteins, which we partially tackled through Cytoscape.

Merging both proteomics and transcriptomics data sets allowed us to graph a detailed map of the CA differential interactome (Supplementary Figure 1, Supporting Information). The resulting map could be further dissected in 4 subgroups, namely (A) Nfkβ-related pathways; (B) solute carriers (Vitamin carriers such as SCL23A2); (C) glycolytic metabolism (PGM1, LDH, ENO3, GPDH); and (D) muscle stress (protein oxidation) and contraction (Lipoxygenase; thioredoxin 2, glutaredoxin). It is immediately evident that the very heart of the map, harboring a series of transcription factors, is mainly characterized by white nodes, that is to say proteins missing in the submitted data set. However, it should be considered that only differentially expressed proteins and gene transcripts were included in the present analysis. Inclusion of non- or less-significantly differently expressed proteins in the data set would solve this minor issue of the IPA analysis.

The LW interactome exploiting data from the current analysis is presented in Supplementary Figure 2 (Supporting Information). In like fashion to the CA map, the LW interactome could be dissected in 3 subgroups, namely (A) cell growth-related pathways (a series of transcriptional regulators and proliferation-related molecules are present); (B) lipid metabolism/mobilization; (C) muscle growth (myosin isoforms in particular).

The Cytoscape/APID2NET analysis confirmed observations from IPA and revealed two main subgroups of nodes in the CA map, which accounted for proteins devoted to glycolysis (north) and muscle contraction (center, south). Likewise, the LW protein−protein interaction map could be divided in 3 domains, the first including proteins involved in muscle protein

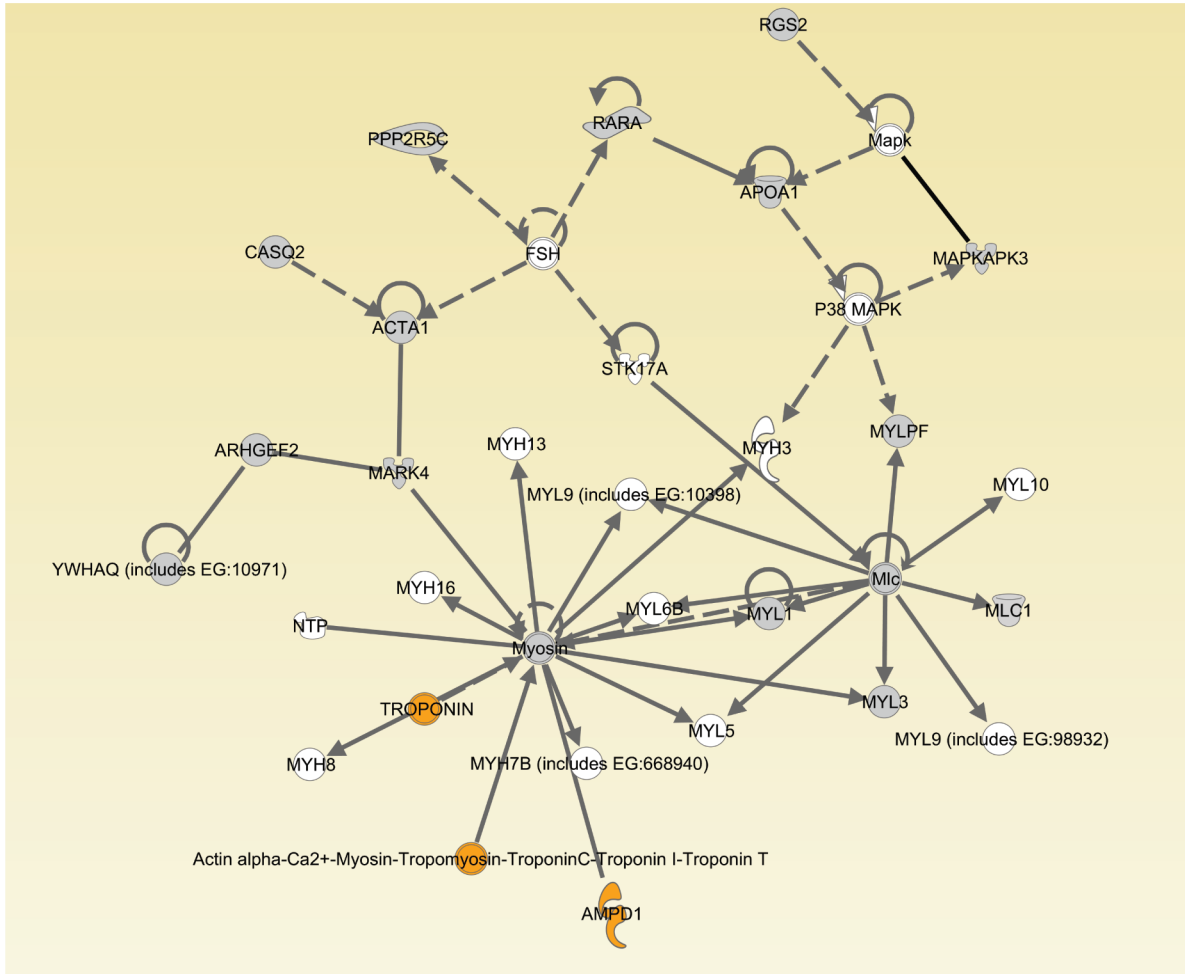

Figure 4. Top network from network analysis via Ingenuity Pathway Analysis in Large White merged protein and microarray data. Gray nodes: proteins from the data set having a match in the database. White nodes: proteins from the database which were not identified (if present) upon the experimental phase. Orange nodes: nondifferentially expressed protein molecules. Gray edges: interactions within a network. Continuous line - edge: direct interaction. Interrupted line - edge: indirect interaction.

synthesis and degradation (north), in muscle contraction the second (south), and lipid mobilization (center).

A detailed discussion of the main proteins/gene transcripts which emerged upon pathway, network and functional GO analyses is provided as follows.

Casertana: Glycolysis, Vitamin Transport and Fat Deposition. CA pig breed is certainly the most precious among Italian breeds, being able to provide large amounts of fat.[40] A detail of the top score network ("Small molecule biochemistry, Metabolism") from network analysis through IPA is given in Figure 3.

As pathway and functional analyses have pointed out, most of the proteins and gene transcripts individuated in CA *longissimus* muscle accounted for metabolic functions. It is worthwhile to underline that glycolytic enzymes or glycolysis-related proteins (PGM1, KHK, GPDH, TPI, ENO3, LDH, CK-M) were individuated through both proteomics and transcriptomics approaches.

Glycolysis is the major metabolic pathway that provides cells with metabolic precursors and a rapid source of energy. Following the glycolytic order, phosphoglucomutase (PGM), ketohexokinase (KHK), glycerol-3-phosphate dehydrogenase (GPDH) and triosephosphate isomerase (TPI) are closely involved in shifts in the main pathway of glycolysis.

Glycerol-phosphate dehydrogenase (GPDH) catalyzes the conversion of glycerol-3- phosphate into the glycolytic intermediary DHAP and viceversa. Working in the former direction this enzyme constitutes a positive switch for glycolysis, while in the latter it produces glycerol-3 phosphate which could be exploited to esterify fatty acids in order to form triglycerides.[41] Indeed, the requirement for net balance of synthesis, degradation and transport for all intermediates in the pathways from glucose to fat imposes constraints on the balance of fluxes between different pathways.[15] The central role of GPDH in the triglyceride synthesis makes this enzyme a useful marker of late adipogenesis extensively used in mammals.[42] This is in agreement with the marked tendency in Casertana to accumulate a fat mass.

The triosephosphate isomerase (TPI) enzyme functions at a metabolic cross-road ensuring the rapid equilibration of the triosephosphates produced by aldolase in glycolysis, which is interconnected to lipid metabolism, to glycerol-3-phosphate shuttle and to the pentose phosphate pathway.[43] TPI connection to lipid metabolism has been suggested to positively relate with a tender meat.[44]

Pig muscle enolase 3 (ENO3) has been thoroughly investigated over the last decades.[45] ENO is a metalloenzyme respon-

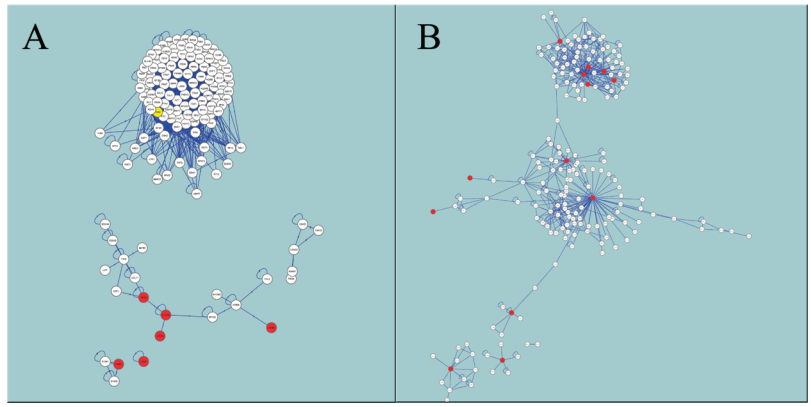

Figure 5. Network analysis of differentially-expressed proteins in (A) Casertana and (B) Large White through Cytoscape/APID2NET. This analysis confirms observations of the whole data set through Ingenuity Pathway Analysis (Supplementary Figure 1) and reveals two main subgroups of nodes in the Casertana map, which account for proteins devoted to glycolysis (north) and Muscle contraction (center, south). Likewise, the Large White protein−protein interaction map could be divided in 3 domains (Supplementary Figure 2), the first including proteins involved in muscle protein synthesis and degradation (north), in muscle contraction the second (south), and lipid mobilization (center).

sible for the catalysis of 2-phosphoglycerate to phosphoenolpyruvate, the ninth and penultimate step of glycolysis.

Various isoforms of ENO have been shown to have a greater abundance in pigs accumulating more intramuscular fat, both within a commercial population[4] and between breeds.[15,16] Gender and rearing conditions also influence several glycolytic enzymes including ENO3.[15,16]

ENO correlation with creatine kinase-M (CK-M) has been observed *in vitro*, suggestive of a likely role in the modulation of glycolytic metabolism.[46,48]

It has been suggested that the CK-system has been positively selected during evolution since it could provide an advantage in the search of food and to escape from predators.[49] Interestingly, CK-M, along with myoglobin, is also a marker of muscular damage, thus it is also used as a suitable marker for heart infarction.[50] Myoglobin has been found to be overexpressed in CA muscle as well.

Generally, a high myoglobin concentration in muscle is associated with a high level of muscular activity and high capability for aerobic metabolism.[51] High levels of myoglobin and mitochondria are believed to exist in slow twitch oxidative fibers.[52] This is partly in contrast with the fast-twitch glycolytic nature of the *longissimus* muscle and with the glycolytic-oriented molecular behavior outlined by functional analysis results. Nevertheless, this is coherent with previous observations about a direct correlation of M-CK, myoglobin, GPDH and lactate dehydrogenase (LDH) with outdoor rearing of pig breeds,[16] as it is the case of CA breeds. Moreover, even if high levels of myoglobin and mitochondria are believed to exist in slow oxidative fibers, Takemasa and colleagues have shown that myoglobin can be considerably richer in some fast type fibers.[53]

LDH converts pyruvate to lactate and indicates the anaerobic-glycolytic capacity in muscles. LDH has been reported to increase its expression in a model of adipogenesis induced through peroxisome proliferator-activated receptor γ (PPARγ) activation.[54]

Nonetheless, this is not totally unexpected, as previous observations on high fat deposition breeds did not show to correlate with PPARγ expression changes.[4] In this respect, Nuclear receptor subfamily 1, group H, member 3 (NR1H3) is known to take part in PPAR cascades and induce cholesterol and fat accumulation.[55,56]

Other up-regulated proteins in CA might be related with adipogenesis, mainly transcription factors such as cAMP responsive element modulator and hydroxysteroid dehydrogenase, which both have been shown to induce adipogenesis in 3T3-L1 preadipocytes.[57−59]

High fat accumulation physiological behaviors are highly correlated with an increased risk of lipid peroxidation and inflammatory cascades.[60,61] In this respect, the role of Nfkβ-mediated pathways is relevant in combating inflammation,[60] antagonizing PPAR cascades,[62] in agreement with network analysis observation of CA data (Figure 3).

Negative regulation of NFkβ signaling would result in triggering on the adipogenetic cascades. Therefore, it is notably that gene transcripts for NFKB inhibitor interacting Raslike 1 (NKIRAS1) and COMMD have been individuated as overexpressed in CA.[63]

COMMD proteins terminate NFkβ-mediated transcriptional responses by destabilizing the interaction between NFkβ and its binding sites on chromatin.[64] Therefore, although proteins involved in PPAR cascades are only partially overexpressed, Nfkβ negative regulation could reduce antagonism of PPAR pathways and thus switch on pro-adipogenetic cascades.

The presence of SLC23A2, a specific carrier for glucose and ascorbic acid cellular intake, could be pivotal, as pinpointed by functional analyses (GO terms: vitamin metabolic process, L-ascorbic acid metabolic process). Indeed, if on the one hand glucose uptake could be related to the glycolytic-centered metabolism of CA pigs, ascorbate uptake could be related to protection against oxidative stress, since ascorbate is an antioxidant, mainly tackling lipid and protein peroxidations.[65,66] Analogous function could be played by thioredoxins and glutaredoxins, which have been already related to lipid mediated inflammation, oxidative stress and nuclear transcription signaling cascades.[67−70]

Large White: Lipid Mobilization, Protein Synthesis and Proliferation Pathway for a Constant Growth and Low Fat Deposition. LW pigs, characterized by large size, represent a rugged and hardy breed that can withstand variations in climate and other environmental factors. Their ability to cross with and improve other breeds has given them a leading role in commercial pig production systems and breeding pyramids around the world.

While the LW was originally developed as an active and outdoor breed, they do very well in intensive production systems. LW pigs excel in growth rate and lean meat percentage. These main characteristics were reflected in LW molecular proteomics and transcriptional profiles, as emerged from pathway, functional and network analyses. As for the latter, a detail of the top score network ("Skeletal and muscular system development and functioning, tissue morphology") from network analysis through IPA is given in Figure 4.

At a rapid glance, proteomics data clearly hint at a differential modulation of muscle fiber content in LW pigs when compared against CA (e.g., several myosin light chain isoforms, actin; calsequestrin, muscle contraction). None of the experimental approaches reported in the present study (both proteomics and transcriptomics analyses) individuated any significant difference between CA and LW pig muscles, as far as myosin heavy chains are concerned. This is suggestive of a likely fine-tuning through modulation of myosin light chain isoforms in muscle fibers from these breeds, instead of a dramatic structural reorganization. Fiber composition largely affects muscle properties and thus meat quality.[14] For example, myosin light chain 2 modulates calcium-sensitive cross-bridge transitions in vertebrate skeletal muscle,[71] thus influencing contraction properties of the muscle. Although they are transcribed from two different widely spaced promoters, myosin light chain 1f and 3 definitely share their biological function and are extremely evolutionary conserved in all vertebrates, from mammals to birds,[72] where they contribute to the modulation of the maximal shortening velocity and power output of the muscle.[73,74] In humans, a transcriptome analysis on control patients (body fat 14.6% $\pm$ 4.3 standard deviation) versus endurance athletes (body fat 11.2% $\pm$ 2.2) clearly shows how skeletal muscles from athletes display higher levels of myosin light chain 2 (as in our Large White pigs) and lower levels of glycolytic enzymes (such as, for example, enolase 3).[75] Notably enough, it is known from literature that differential phosphorylation of myosin light chain 2 is fundamental in regulating muscle contraction properties: based on the introduction of negative charges by phosphorylation, it has been hypothesized that the cross-bridges move away from the filament backbone, thus increasing the probability of attachment and force generation.[76] Intriguingly, ProQ Diamond Staining evidenced abundant phosphorylation for myosin light chain (Figure 2) from 2DE gels in LW.

Accordingly, it is long known that alpha-actin positively correlates with synthesis of muscle fiber proteins and, ultimately, with muscle growth.[77] Since Approximately 50% of the protein content of the muscle fiber is made up of the contractile machinery, mostly consisting of myosin complexes of the thick filaments and actin strings of the thin filaments, the upregulation of ACTA1 in LW LM is completely coherent with the greater tendency to mass accumulation of the breed. ACTA1 is indirectly modulated by MYLPF, whose overexpression in LW has been individuated through proteomics approaches.[78] Coherently, calsequestrin (CASQ1) overexpression in LW suggests for an increased need for fine-tuning of calcium-homeostasis, which guarantees proper muscle excitation-contraction-relaxation cycles, even in presence of higher muscular mass.[79] In agreement, CASQ1 is found to diminish its expression in aging skeletal muscles.[80]

Skeletal muscle mass is a balance between protein synthesis and degradation. An imbalance such that proteolysis prevails over synthesis is associated with skeletal muscle atrophy. Along with other muscle homeostasis regulators, LW overexpresses a Serpine Peptidase inhibitor 3 (SERPINA3).[81]

Besides, the overexpression of noncanonical proteins has been correlated with muscle functioning modulation and myogenesis as well. For example, rho/rac guanine nucleotide exchange factor (ARHGEF) is a guanine nucleotide exchange factor for Rho whose activity is regulated through a cycle of microtubule binding and release. Phosphorylation of ARHGEF at Ser(885) by PAK1 induces 14-3-3 (YWHAQ in Figure 3) binding to the exchange factor and relocation of 14-3-3 to microtubules.[82] The 14-3-3 protein γ is member of the 14-3-3 protein family, which are conserved regulatory proteins that bind to a multitude of functionally diverse signaling proteins including kinases and phophatases.[83] It has been proposed that the 14-3-3 proteins have a role in the regulation of myosin light chain kinase that becomes phosphorylated during muscle contraction, and it can be speculated that 14-3-3 protein may play a role in the muscle contraction during rigor.[84] ARHGEF also binds to MARK4,[85] which is known to modulate actin cytoskeleton in cell polarity and cell structural development.[86]

As one of the peculiar characteristics of LW breeds is their constant growth during their lifespan, it is not unexpected that both pathway and network analyses stressed the role of several proteins/gene transcripts involved in cell cycle regulation and proliferation control. One of these is PPP2R5C, of the phosphatase 2A regulatory subunit B family. PPP2R5C is one of the four major Ser/Thr phosphatases, and it is implicated in the negative control of cell growth and metabolism.[87]

In parallel, LW showed to overexpress RGS2, a simple RGS protein with the potential to integrate multiple signaling networks. Recently, the amino-terminal domain of RGS2 was shown to interact with and regulate three different effector proteins: adenylyl cyclase, tubulin, and the cation channel TRPV6. RGS2 has been associated with the modulation of the thickness of skeletal muscle fibers.[88,89]

Peroxiredoxin 2 (GO: oxygen and reactive oxygen species metabolic process, apoptosis) is a member of the peroxiredoxin family of antioxidant enzymes, which reduce hydrogen peroxide and alkyl hydroperoxides. Its overexpression in LW muscles could be related to cellular growth, as it has been observed that peroxiredoxin 2 can reduce hydrogen peroxide generated in response to growth factors and tumor necrosis factor-alpha.[90]

Downstream of mitogen-activated protein kinases, MAPKAPK3 (MAP kinase kinase) is ubiquitously overexpressed in large Diannan pigs compared to smaller ones.[91] MAPKAPK3 is thought to regulate gene expression at the transcriptional and post-transcriptional level, control cytoskeletal architecture and cell-cycle progression, and are implicated in inflammation.[92]

Estrogen-related receptor alpha (ERRα) was overexpressed in LW pigs. Transcriptional control in LW pigs is not only strictly related to muscular growth, but also in regulation of its metabolism. ERRα has wide tissue distribution but it is most highly expressed in tissue that preferentially use fatty acids as energy sources such as kidney, heart, cerebellum, intestine, and skeletal muscle.[93] ERRα regulates genes involved in mitochondrial biogenesis,[94] gluconeogenesis,[95] oxidative phosphorylation,[96] and fatty acid metabolism.[97] This is relevant in that although displaying higher levels of ERRα transcripts, LW pigs are less prone to adipogenesis. This could be explained when dissecting the pivotal molecules which are indicated by network analyses, in which a high tendency is observed in LW pigs to mobilize and consume lipids instead of increasing their deposi-

tion. Apolipoprotein A1 (APOA1), carnityne carnitine palmitoyltransferase 1C (CPT1C), malic enzyme (ME), and Glyoxalase I perfectly fit in this framework.

CPTI is believed to contribute to the transport of fatty acids across the mitochondrial membranes, an important step in beta-oxidation of long-chain fatty acids, via the carnitine palmitoyltransferase enzyme system.[99] A greater expression of this transporter suggests a larger utilization of long chain fatty acids by LW pigs.

ME catalyzes the reductive carboxylation of pyruvate to malate. The malate can then be oxidized to oxaloacetate, through the catalytic activity of the TCA cycle enzyme, malate dehydrogenase.

Glioxalase I is part of the glyoxalase system present in the cytosol of cells, catalyzing the conversion of reactive, acyclic α-oxoaldehydes like malonic dialdehyde (MDA), a cytosolic aldehyde produced in cells into the corresponding α-hydroxy-acids. The rise of the amount of MDA is associated to lipid peroxidation as well as to cell damage, which is particularly high at the protein level (protein turnover) in fast growing muscle tissues.[99]

Taken together, these observations prompt a series of considerations of a more oxidative-oriented metabolism for this muscle in LW pigs, against an inefficient strict glycolytic tendency of CA ones.

Conclusions

This study was aimed at detecting representative molecules which could be related to the increased fat deposition attitude of the Italian breed and the leanness of the meat of LW pigs. Most of the differentially expressed individuated proteins and gene transcripts account for proteins which have been proposed to play a role in meat quality in literature (Supplementary Figure 3, Supporting Information).[15,16]

CA, the endangered, semiwild fat-type swine, showed to rely on glycolitic enzymes, in contrast with LW, which rather appears to be oriented toward lipid mobilization and oxidation. This is apparently in contrast with well-established reports from literature, indicating that breeds selected for high fat deposition or meat leanness display a tendency toward lipid oxidation or glycolytic metabolic behaviors, respectively.[100] However, it has also been observed that LW breeds, selected for nine generations against backfat thickness and for improved growth rate and feed conversion efficiency displayed higher plasma free fatty acid levels and thus higher lipid mobilization rather than fat deposition, when compared against other lines which had been randomly bred for six generations.[101]

Besides, considering the semiwild rearing environment of CA, the expression of a fast energy source could be related to a greater need of energy compared to a static lifestyle of LW.

Nevertheless, glycolysis is an inefficient way to generate adenosine 5′-triphosphate (ATP), which in turn guarantees a rapid rate of biomass accumulation, resulting in fat deposition in CA pigs.[102]

In LW, the presence of proteins related to mitochondrial activity, lipid mobilization, insulin resistance, and antioxidant protein and transcripts are suggestive of a likely constant mitochondrial activity consuming the smaller fat mass. LW pigs clearly showed a tendency to muscular growth. Most of the overexpressed proteins and transcripts belonged to protein groups composing the fiber and the sarcoplasmic reticulum, as well as with antiproteolytic enzymes, as expected from a breed selected to develop lean muscular mass.

Abbreviations: CA, Casertana; CPT1C, carnitine palmitoyltransferase; CSQ, calsequestrin; GPDH, glycerol-3-phosphate dehydrogenase; IPA, Ingenuity Pathway Analysis; LDH, lactate dehydrogenase; LW, Large White; M-CK, muscle creatine kinase; ME, malic enzyme; PGM1, phosphoglucomutase 1; PPAR, peroxisome proliferator-activated receptor; TPI, triose phosphate isomerase.

Acknowledgment. This study has been supported by the "GENZOOT" research programme, funded by the Italian Ministry of Agriculture. The Authors would like to thank Dr. Bianca Moioli for her stimuli and support.

Supporting Information Available: Supplementary Figure 1. Network analysis of differentially expressed proteins and gene transcripts merged together in Large White through Ingenuity Pathway Analysis. The interactome could be dissected in 4 subgroups, namely Nfkβ-related pathways (A), solute carriers (B), glycolytic metabolism (D) and muscle stress and contraction (D). Supplementary Figure 2. Network analysis of differentially expressed proteins and gene transcripts merged together in Casertana through Ingenuity Pathway Analysis. The interactome could be dissected in 3 subgroups, namely cell growth-related pathways (A), lipid metabolism (B), muscle growth (C). Supplementary Figure 3. Schematic view of the experimentally individuated differentially expressed proteins/gene transcripts in Casertana (CA) and Large White pigs which might influence meat quality, as suggested by Kwasiborski et al.[15,16] This material is available free of charge via the Internet at http://pubs.acs.org.

References

(1) Megens, H. J.; Crooijmans, R. P.; San Cristobal, M.; Hui, X.; Li, N.; Groenen, M. A. Biodiversity of pig breeds from China and Europe estimated from pooled DNA samples: differences in microsatellite variation between two areas of domestication. *Gen. Sel. Evol.* **2008**, *40* (1), 103–128.

(2) Davoli, R.; Braglia, S. Molecular approaches in pig breeding to improve meat quality. *Brief. Funct. Genomic Prot.* **2008**, *6* (4), 313–321.

(3) Xu, Y. J.; Jin, M. L.; Wang, L. J.; Zhang, A. D.; Zuo, B.; Xu, D. Q.; Ren, Z. Q.; Lei, M. G.; Mo, X. Y.; Li, F. E.; Zheng, R.; Deng, C. Y.; Xiong, X. Y. Differential proteome analysis of porcine skeletal muscles between Meishan and Large White. *J. Anim. Sci.* **2009**, *87* (8), 2519–2527.

(4) Liu, J.; Damon, M.; Guitton, N.; Guisle, I.; Ecolan, P.; Vincent, A.; Cherel, P.; Gondret, F. Differentially-expressed genes in pig Longissimus muscles with contrasting levels of fat, as identified by combined transcriptomic, reverse transcription PCR, and proteomic analyses. *J. Agri. Food. Chem.* **2009**, *57* (9), 3808–3817.

(5) Scherf, B. D. *WorldWatch List for Animal Diversity*, 3rd ed.; FAO: Rome, Italy, 2000.

(6) Jones, G. F. Genetic aspects of domestication, common breeds and their origin. In *The Genetics of the Pig*; Ruvinsky, A., Rothschild, M. F., Eds.; CAB International: Oxon, U.K., 1998; pp 17−50.

(7) Larson, G.; Dobney, K.; Albarella, U.; Fang, M.; Matisoo-Smith, E.; Robins, J.; Lowden, S.; Finlayson, H.; Brand, T.; Willerslev, E.; Rowley-Convy, P.; Andersson, L.; Cooper, A. Worldwide phylogeography of wild boar reveals multiple centers of pig domestication. *Science* **2005**, *307*, 1618–1621.

(8) *Handbook to the Breeds of theWorld*; Porter, V., Pigs, A., Eds.; Helm Information Ltd.: Near Robertsbridge, U.K., 1993.

(9) Zullo, A.; Barone, C. M. A.; Colatruglio, P.; Girolami, A.; Matassino, D. Chemical composition of pig meat from the genetic type 'Casertana' and its crossbreeds. *Meat Sci.* **2003**, *63* (1), 89–100.

(10) Pietrolà, E.; Pilla, F.; Maiorano, G.; Matassino, D. Morphological traits, reproductive and productive performances of Casertana pigs reared outdoors. *Ital. J.Anim. Sci.* **2006**, *5*, 139–146.

(11) Kim, N. K.; Joh, J. H.; Park, H. R.; Kim, O. H.; Park, B. Y.; Lee, C. S. Differential expression profiling of the proteomes and their mRNAs in porcine white and red skeletal muscles. *Proteomics* **2004**, *4* (11), 3422–3428.

(12) Wimmers, K.; Murani, E.; Ngu, N. T.; Schellander, K.; Ponsuksili, S. Structural and functional genomics to elucidate the genetic background of microstructural and biophysical muscle properties in the pig. *J. Anim. Breed. Genet.* **2007**, *124* (1), 27–34.
(13) Quiroz-Rothe, E.; Rivero, J. L. Coordinated expression of myosin heavy chains, metabolic enzymes, and morphological features of porcine skeletal muscle fiber types. *Microsc. Res. Tech.* **2004**, *65* (1−2), 43–61.
(14) Toniolo, L.; Patruno, M.; Maccatrozzo, L.; Pellegrino, M. A.; Canepari, M.; Rossi, R.; D'Antona, G.; Bottinelli, R.; Reggiani, C.; Mascarello, F. Fast fibres in a large animal: fibre types, contractile properties and myosin expression in pig skeletal muscles. *J. Exp. Biol.* **2004**, *207* (11), 1875–1886.
(15) Kwasiborski, A.; Sayd, T.; Chambon, C.; Santé-Lhoutellier, V.; Rocha, D.; Terlouw, C. Pig Longissimus lumborum proteome: Part I. Effects of genetic background, rearing environment and gender. *Meat Sci.* **2008**, *80*, 968–981.
(16) Kwasiborski, A.; Sayd, T.; Chambon, C.; Santé-Lhoutellier, V.; Rocha, D.; Terlouw, C. Pig Longissimus lumborum proteome: Part II: Relationships between protein content and meat quality. *Meat Sci.* **2008**, *80*, 982–996.
(17) Hoogland, C.; Mostaguir, K.; Sanchez, J.-C.; Hochstrasser, D.; Appel, R. D. SWISS-2DPAGE, ten years later. *Proteomics* **2004**, *4* (8), 2352–2356.
(18) Bradford, M. M. A rapid and sensitive method for the quantitation of microgram quantities of protein utilizing the principle of protein-dye binding. *Anal. Chem.* **1976**, *72*, 248–254.
(19) Talamo, F.; D'Ambrosio, C.; Arena, S.; Del Vecchio, P.; Ledda, L.; Zehender, G.; Ferrara, L.; Scaloni, A. Proteins from bovine tissues and biological fluids: Defining a reference electrophoresis map for liver, kidney, muscle, plasma and red blood cells. *Proteomics* **2003**, *3*, 440–460.
(20) Beresini, M. H.; Sugarman, B. J.; Shepard, H. M.; Epstein, L. B. Synergistic induction of polypeptides by tumor necrosis factor and interferon-γ in cells sensitive or resistant to tumor necrosis factor: Assessment by computer based analysis of two-dimensional gels using the PDQUEST system. *Electrophoresis* **1990**, *11*, 232–241.
(21) Shevchenko, A.; Wilm, M.; Vorm, O.; Mann, M. Mass Spectrometric Sequencing of Proteins from Silver-Stained Polyacrylamide Gels. *Anal. Chem.* **1996**, *68*, 850–858.
(22) D'Amici, G. M.; Timperio, A. M.; Zolla, L. Coupling of Native Liquid Phase Isoelectrofocusing and Blue Native Polyacrylamide Gel Electrophoresis: A Potent Tool for Native Membrane Multiprotein Complex Separation. *J. Proteome Res.* **2008**, *7*, 1326–1330.
(23) Peng, X.; Wood, C.; Blalock, E.; Chen, K.; Landfield, P.; Stromberg, A. Statistical implications of pooling RNA samples for microarray experiments. *BMC Bioinf.* **2003**, *4* (1), 26.
(24) Kendziorski, C.; Irizarry, R. A.; Chen, K. S.; Haag, J. D.; Gould, M. N. On the utility of pooling biological samples in microarray experiments. *Proc. Natl. Acad. Sci. U.S.A.* **2005**, *102* (12), 4252–4257.
(25) Dobbin, K. K.; Kawasaki, E. S.; Peterson, D. W.; Simon, R. M. Characterizing dye bias in microarray experiments. *Gene expression* **2005**, *21* (10), 2430–2437.
(26) Naidoo, S.; Denby, K. J.; Berger, D. K. Microarray experiments: considerations for experimental design. *S. Afr. J. Sci.* **2005**, *101*, 347–354.
(27) Fang, Y. A.; Hoyle, D. C.; Hayes, A.; Bashein, A.; Oliver, S. G.; Waddington, D.; Rattray, M. A model-based analysis of microarray experimental error and normalisation. *Nucleic Acids Res.* **2003**, *31* (16), e96.
(28) D'Alessandro, A.; Righetti, P. G.; Zolla, L. The Red Blood Cell proteome and interactome: an update. *J. Proteome Res.* **2010**, *9* (1), 144–163.
(29) Timperio, A. M.; D'Alessandro, A.; Pariset, L.; D'Amici, G. M.; Valentini, A.; Zolla, L. Comparative proteomics and transcriptomics analyses of livers from two different Bos taurus breeds: Chianina and Holstein Friesian. *J. Proteomics* **2009**, *73* (2), 309–322.
(30) IPA (Ingenuity Systems, www.ingenuity.com).
(31) Shannon, P.; Markiel, A.; Ozier, O.; Baliga, N. S.; Wang, J. T.; Ramage, D.; Amin, N.; Schwikowski, B.; Ideker, T. Cytoscape: a software environment for integrated models of biomolecular interaction networks. *Gen. Res.* **2003**, *13* (11), 2498–2504.
(32) Hernandez-Toro, J.; Prieto, C.; De Las Rivas, J. APID2NET: unified interactome graphic analyzer. *Bioinformatics* **2007**, *23* (18), 2495–2497.
(33) Al-Shahrour, F.; Minguez, P.; Tárraga, J.; Medina, I.; Alloza, E.; Montaner, D.; Dopazo, J. FatiGO+: a functional profiling tool for genomic data. Integration of functional annotation, regulatory motifs and interaction data with microarray experiments. *Nucleic Acids Res.* **2007**, *35*, 91–96.
(34) Al-Shahrour, F.; Minguez, P.; Vaquerizas, J. M.; Conde, L.; Dopazo, J. BABELOMICS: a suite of web-tools for functional annotation and analysis of group of genes in high-throughput experiments. *Nucleic Acids Res.* **2005**, *33*, 460–464.
(35) Al-Shahrour, F.; Díaz-Uriarte, R.; Dopazo, J. FatiGO: a web tool for finding significant associations of Gene Ontology terms with groups of genes. *Bioinformatics* **2004**, *20*, 578–580.
(36) Hornshøj, H.; Bendixen, E.; Conley, L. N.; Andersen, P. K.; Hedegaard, J.; Panitz, F.; Bendixen, C. Transcriptomic and proteomic profiling of two porcine tissues using high-throughput technologies. *BMC Gen.* **2009**, *10*, 30.
(37) Nie, L.; Wu, G.; Culley, D. E.; Schotten, J. C. M.; Zhang, W. Integrative Analysis of Transcriptomic and Proteomic Data: Challenges, Solutions and Applications. *Crit. Rev. Biotechnol.* **2007**, *27* (2), 63–75.
(38) Samulin, J.; Berget, I.; Lien, S.; Sundvold, H. Differential gene expression of fatty acid binding proteins during porcine adipogenesis. *Comp. Biochem. Physiol. B: Biochem. Mol. Biol.* **2008**, *151* (2), 147–152.
(39) Maier, T.; Güell, M.; Serrano, L. Correlation of mRNA and protein in complex biological samples. *FEBS Lett.* **2009**, *583* (24), 3966–73.
(40) Salvaterra, M. Agraria.org - Agrarian instruction online Italian breeds of livestock; 2000; http://eng.agraria.org/.
(41) Fell, D. A.; Small, J. R. Fat synthesis in adipose tissue. An examination of stoichiometric constraints. *Biochem. J.* **1986**, *238* (3), 781–786.
(42) Salazar-Olivo, L. A.; Castro-Muñozledo, F.; Kuri-Harcuch, W. A preadipose 3T3 cell variant highly sensitive to adipogenic factors and to human growth hormone. *J. Cell Sci.* **1995**, *108* (5), 2101–2107.
(43) Orosz, F.; Oláh, J.; Ovádi, J. Triosephosphate isomerase deficiency: New insights into an enigmatic disease. *Biochim. Biophys. Acta* **2009**, *1792* (12), 1168–1174.
(44) Laville, E.; Sayd, T.; Terlouw, C.; Chambon, C.; Damon, M.; Larzul, C.; Leroy, P.; Glénisson, J.; Chérel, P. Comparison of sarcoplasmic proteomes between two groups of pig muscles selected for shear force of cooked meat. *J. Agric. Food. Chem.* **2007**, *55* (14), 5834–5841.
(45) Farrar, W. W.; Deal, W. C., Jr. Purification and properties of pig liver and muscle enolases. *J. Protein Chem.* **1995**, *14* (6), 487–497.
(46) Merkulova, T.; Lucas, M.; Jabet, C.; Lamandé, N.; Rouzeau, J. D.; Gros, F.; Lazar, M.; Keller, A. Biochemical characterization of the mouse muscle-specific enolase:developmental changes in electrophoretic variants and selective binding to other proteins. *Biochem. J.* **1997**, *323* (3), 791–800.
(47) Foucault, G.; Vacher, M.; Cribier, S.; Arrio-Dupont, M. Interactions between beta-enolase and creatine kinase in the cytosol of skeletal muscle cells. *Biochem. J.* **2000**, *346* (1), 127–131.
(48) Wallimann, T.; Wyss, M.; Brdiczka, D.; Nicolay, K.; Eppenberger, H. M. Intracellular compartmentation, structure and function of creatine kinase isoenzymes in tissues with high and fluctuating energy demands: the 'phosphocreatine circuit' for cellular energy homeostasis. *Biochem. J.* **1992**, *281* (1), 21–40.
(49) Ventura-Clapier, R.; Kaasik, A.; Veksler, V. Structural and functional adaptations of striated muscles to CK deficiency. *Mol. Cell. Biochem.* **2004**, *257*, 29–41.
(50) McComb, J. M.; McMaster, E. A.; MacKenzie, G.; Adgey, A. A. Myoglobin and creatine kinase in acute myocardial infarction. *Br. Heart J.* **1984**, *51* (2), 189–194.
(51) *Meat science*, 6th ed.; Lawrie, R. A., Ed.; Woodhead Publishing: New York, 1998; pp 43−73.
(52) Takemasa, T.; Sugimoto, K.; Miyazaki, M.; Machida, M.; Ikeda, S.; Hitomi, Y.; Kizaki, T.; Ohno, H.; Yamashita, K.; Haga, S. Simple method for the identification of oxidative fibers in skeletal muscle. *Eur. J. Appl. Physiol.* **2004**, *91* (2−3), 357–359.
(53) Ordway, G. A.; Garry, D. Myoglobin: an essential hemoprotein in striated muscle. *J. Exp. Biol.* **2004**, *207*, 3441–3446.
(54) Mueller, E.; Drori, S.; Aiyer, A.; Yie, J.; Sarraf, P.; Chen, H.; Hauser, S.; Rosen, E. D.; Ge, K.; Roeder, R. G.; Spiegelman, B. M. Genetic analysis of adipogenesis through peroxisome proliferator-activated receptor γ isoforms. *J. Biol. Chem.* **2002**, *277* (44), 41925–41930.
(55) Cummins, C. L.; Volle, D. H.; Zhang, Y.; McDonald, J. G.; Sion, B.; Lefrançois-Martinez, A. M.; Caira, F.; Veyssière, G.; Mangelsdorf, D. J.; Lobaccaro, J. M. Liver X receptors regulate adrenal cholesterol balance. *J. Clin. Invest.* **2006**, *116* (7), 1902–1912.

(56) Xu, C.; Li, C. Y.; Kong, A. N. Induction of phase I, II and III drug metabolism/transport by xenobiotics. *Arch. Pharm. Res.* **2005**, *28* (3), 249–268.
(57) Reusch, J. E.; Colton, L. A.; Klemm, D. J. CREB activation induces adipogenesis in 3T3-L1 cells. *Mol. Cell. Biol.* **2000**, *20* (3), 1008–1020.
(58) Vankoningsloo, S.; De Pauw, A.; Houbion, A.; Tejerina, S.; Demazy, C.; de Longueville, F.; Bertholet, V.; Renard, P.; Remacle, J.; Holvoet, P.; Raes, M; Arnould, T. CREB activation induced by mitochondrial dysfunction triggers triglyceride accumulation in 3T3-L1 preadipocytes. *J. Cell. Sci.* **2006**, *119* (7), 1266–1282.
(59) Bujalska, I. J.; Gathercole, L. L.; Tomlinson, J. W.; Darimont, C.; Ermolieff, J.; Fanjul, A. N.; Rejto, P. A.; Stewart, P. M. A novel selective 11beta-hydroxysteroid dehydrogenase type 1 inhibitor prevents human adipogenesis. *J. Endocrinol.* **2008**, *197* (2), 297–307.
(60) Ringseis, R.; Piwek, N.; Eder, K. Oxidized fat induces oxidative stress but has no effect on NF-kappaB-mediated proinflammatory gene transcription in porcine intestinal epithelial cells. *Inflamm. Res.* **2007**, *56* (3), 118–125.
(61) Galili, O.; Versari, D.; Sattler, K. J.; Olson, M. L.; Mannheim, D.; McConnell, J. P.; Chade, A. R.; Lerman, L. O.; Lerman, A. Early experimental obesity is associated with coronary endothelial dysfunction and oxidative stress. *Am. J. Physiol. Heart. Circ. Physiol.* **2007**, *292* (2), H904–911.
(62) Suzawa, M.; Takada, I.; Yanagisawa, J.; Ohtake, F.; Ogawa, S.; Yamauchi, T.; Kadowaki, T.; Takeuchi, Y.; Shibuya, H.; Gotoh, Y.; Matsumoto, K.; Kato, S. Cytokines suppress adipogenesis and PPAR-gamma function through the TAK1/TAB1/NIK cascade. *Nat. Cell Biol.* **2003**, *Mar;5* (3), 224–230.
(63) Huxford, T.; Ghosh, G. Inhibition of transcription factor NF-kappaB activation by kappaB-Ras. *Met. Enzymol.* **2006**, *407*, 527–534.
(64) Maine, G. N.; Burstein, E. COMMD proteins: COMMing to the scene. *Cell. Mol. Life Sci.* **2007**, *64* (15), 1997–2005.
(65) Dragsted, L. O. Biomarkers of exposure to vitamins A, C, and E and their relation to lipid and protein oxidation markers. *Eur. J. Nutr.* **2008**, *47* (2), 3–18.
(66) Voss, P.; Engels, M.; Strosova, M.; Grune, T.; Horakova, L. Protective effect of antioxidants against sarcoplasmic reticulum (SR) oxidation by Fenton reaction, however without prevention of Ca-pump activity. *Toxicol. In Vitro* **2008**, *22* (7), 1726–1733.
(67) Fernandez-Robredo, P.; Moya, D.; Rodriguez, J. A.; Garcia-Layana, A. Vitamins C and e reduce retinal oxidative stress and nitric oxide metabolites and prevent ultrastructural alterations in porcine hypercholesterolemia. *Invest. Ophthalmol. Vis. Sci.* **2005**, *46* (4), 1140–1146.
(68) May, J. M.; Morrow, J. D.; Burk, R. F. Thioredoxin reductase reduces lipid hydroperoxides and spares alpha-tocopherol. *Biochem. Biophys. Res. Commun.* **2002**, *292* (1), 45–49.
(69) Kumar, S.; Holmgren, A. Induction of thioredoxin, thioredoxin reductase and glutaredoxin activity in mouse skin by TPA, a calcium ionophore and other tumor promoters. *Carcinogenesis* **1999**, *20* (9), 1761–1767.
(70) Marumoto, M.; Suzuki, S.; Hosono, A.; Arakawa, K.; Shibata, K.; Fuku, M.; Goto, C.; Tokudome, Y.; Hoshino, H.; Imaeda, N.; Kobayashi, M.; Yodoi, J.; Tokudome, S. Changes in thioredoxin concentrations: an observation in an ultra-marathon race. *Environ. Health Prev. Med.* **2010**, *15* (3), 129–134.
(71) Metzger, J. M.; Moss, R. L. Myosin light chain 2 modulates calcium-sensitive cross-bridge transitions in vertebrate skeletal muscle. *Biophys. J.* **1992**, *63* (2), 460–468.
(72) Strehler, E. E.; Periasamy, M.; Strehler-Page, M. A.; Nadal-Ginard, B. Myosin light-chain 1 and 3 gene has two structurally distinct and differentially regulated promoters evolving at different rates. *Mol. Cell. Biol.* **1985**, *5* (11), 3168–3182.
(73) Moss, R. L.; Diffee, G. M.; Greaser, M. L. Contractile properties of skeletal muscle fibers in relation to myofibrillar protein isoforms. *Rev. Physiol. Biochem. Pharmacol.* **1995**, *126*, 1–63.
(74) Bicer, S.; Reiser, P. J. Myosin light chain isoform expression among single mammalian skeletal muscle fibers: species variations. *J. Musc. Res. Cell. Mot.* **2004**, *25*, 623–633.
(75) Yoshioka, M.; Tanaka, H.; Shono, N.; Snyder, E. E.; Shindo, M.; St-Amand, J. Serial analysis of gene expression in the skeletal muscle of endurance athletes compared to sedentary men. *FASEB J.* **2003**, *17* (13), 1812–1819.
(76) Barany, K.; Barany, M.; Gillis, J. M.; Kushmerick, M. J. Phosphorylation-dephosphorylation of the 18,000-dalton light chain of myosin during the contraction-relaxation cycle of frog muscle. *J. Biol. Chem.* **1979**, *254*, 3617–3623.
(77) Helferich, W.; Jump, D. B.; Anderson, D. B.; Skjaerlund, D. M.; Merkel, R. A.; Bergen, W. G. Skeletal muscle alpha-actin synthesis is increased pretranslationally in pigs fed the phenethanolamine ractopamine. *Endocrinology* **1990**, *126* (6), 3096–3100.
(78) Juliano, R. L. Signal transduction by cell adhesion receptors and the cytoskeleton: functions of integrins, cadherins, selectins, and immunoglobulin-superfamily members. *Annu. Rev. Pharmacol. Toxicol.* **2002**, *42*, 283–323.
(79) Murray, B. E.; Froemming, G. R.; Maguire, P. B.; Ohlendieck, K. Excitation-contraction-relaxation cycle: role of Ca2+-regulatory membrane proteins in normal, stimulated and pathological skeletal muscle (review). *Int. J. Mol. Med.* **1998**, *1* (4), 677–687.
(80) O'Connell, K.; Gannon, J.; Doran, P.; Ohlendieck, K. Reduced expression of sarcalumenin and related Ca2+ -regulatory proteins in aged rat skeletal muscle. *Exp. Gerontol.* **2008**, *43* (10), 958–961.
(81) Akaaboune, M.; Verdière-Sahuqué, M.; Lachkar, S.; Festoff, B. W.; Hantaï, D. Serine proteinase inhibitors in human skeletal muscle: expression of beta-amyloid protein precursor and alpha 1-anti-chymotrypsin in vivo and during myogenesis in vitro. *J. Cell. Physiol.* **1995**, *165* (3), 503–511.
(82) Zenke, F. T.; Krendel, M.; DerMardirossian, C.; King, C. C.; Bohl, B. P.; Bokoch, G. M. p21-activated kinase 1 phosphorylates and regulates 14−3-3 binding to GEF-H1, a microtubule-localized Rho exchange factor. *J. Biol. Chem.* **2004**, *279* (18), 18392–18400.
(83) Fu, H. Subramanian RR, Masters SC. 14−3-3 proteins: structure, function, and regulation. *Annu. Rev. Pharmacol. Toxicol.* **2000**, *40*, 617–647.
(84) Lametsch, R.; Kristensen, L.; Larsen, M. R.; Therkildsen, M.; Oksbjerg, N.; Ertbjerg, P. Changes in the muscle proteome after compensatory growth in pigs. *J. Anim. Sci.* **2006**, *84* (4), 918–924.
(85) Brajenovic, M.; Joberty, G.; Küster, B. Bouwmeester T, Drewes G. Comprehensive proteomic analysis of human par protein complexes reveals an interconnected protein network. *J. Biol. Chem.* **2004**, *279* (13), 12804–12811.
(86) Trinczek, B.; Brajenovic, M.; Ebneth, A.; Drewes, G. MARK4 Is a Novel Microtubule-associated Proteins/Microtubule Affinity-regulating Kinase That Binds to the Cellular Microtubule Network and to Centrosomes. *J. Biol. Chem.* **2004**, *279* (7), 5915–5923.
(87) McCright, B.; Virshup, D. M. Identification of a new family of protein phosphatase 2A regulatory subunits. *J. Biol. Chem.* **1995**, *270* (44), 26123–26128.
(88) Heximer, S. P.; Blumer, K. J. RGS proteins: Swiss army knives in seven-transmembrane domain receptor signaling networks. *Sci. STKE* **2007**, *370*, pe2.
(89) Wu, C.; Zeng, Q.; Blumer, K. J.; Muslin, A. J. RGS proteins inhibit Xwnt-8 signaling in Xenopus embryonic development. *Development* **2000**, *127* (13), 2773–2784.
(90) Kang, S. W.; Chae, H. Z.; Seo, M. S.; Kim, K.; Baines, I. C.; Rhee, S. G. Mammalian peroxiredoxin isoforms can reduce hydrogen peroxide generated in response to growth factors and tumor necrosis factor-alpha. *J. Biol. Chem.* **1998**, *273* (11), 6297–6302.
(91) Yonggang, L. A novel porcine gene, MAPKAPK3, is differentially expressed in the pituitary gland from mini-type Diannan small-ear pigs and large-type Diannan small-ear pigs. *Mol. Biol. Rep.* **2010**, *37* (7), 3345–3349.
(92) Gaestel, M. MAPKAP kinases - MKs - two's company, three's a crowd. *Nat. Rev. Mol. Cell. Biol.* **2006**, *7* (2), 120–130.
(93) Wu, Z.; Puigserver, P.; Andersson, U.; Zhang, C.; Adelmant, G.; Mootha, V.; Troy, A.; Cinti, S.; Lowell, B.; Scarpulla, R. C.; Spiegelman, B. M. Mechanisms controlling mitochondrial biogenesis and respiration through the thermogenic coactivator PGC-1. *Cell* **1999**, *98* (1), 115–124.
(94) Yoon, J. C.; Puigserver, P.; Chen, G.; Donovan, J.; Wu, Z.; Rhee, J.; Adelmant, G.; Stafford, J.; Kahn, C. R. Granner DK, Newgard CB, Spiegelman BM. Control of hepatic gluconeogenesis through the transcriptional coactivator PGC-1. *Nature* **2001**, *413* (6852), 131–138.
(95) Mootha, V. K.; Handschin, C.; Arlow, D.; Xie, X.; St Pierre, J.; Sihag, S.; Yang, W.; Altshuler, D.; Puigserver, P.; Patterson, N.; Willy, P. J.; Schulman, I. G.; Heyman, R. A.; Lander, E. S.; Spiegelman, B. M. Erralpha and Gabpa/b specify PGC-1alpha-dependent oxidative phosphorylation gene expression that is altered in diabetic muscle. *Proc. Natl. Acad. Sci. U.S.A.* **2004**, *101* (17), 6570–6575.
(96) Huss, J. M.; Torra, I. P.; Staels, B.; Giguère, V.; Kelly, D. P. Estrogen-related receptor alpha directs peroxisome proliferator-activated receptor alpha signaling in the transcriptional control of energy metabolism in cardiac and skeletal muscle. *Mol. Cell. Biol.* **2004**, *24* (20), 9079–9091.

(97) Luo, J.; Sladek, R.; Carrier, J.; Bader, J. A.; Richard, D.; Giguère, V. Reduced fat mass in mice lacking orphan nuclear receptor estrogen-related receptor alpha. *Mol. Cell. Biol.* **2003**, *23* (22), 7947–7956.
(98) Berthon, P. M.; Howlett, R. A.; Heigenhauser, G. J.; Spriet, L. L. Human skeletal muscle carnitine palmitoyltransferase I activity determined in isolated intact mitochondria. *J. Appl. Physiol.* **1998**, *85* (1), 148–153.
(99) Chuanxi, C. S.; Weisleder, N.; Ko, J. K.; Komazaki, S.; Sunada, Y.; Nishi, M.; Takeshima, H.; Ma, J. Membrane Repair Defects in Muscular Dystrophy Are Linked to Altered Interaction between MG53, Caveolin-3, and Dysferlin. *J. Biol. Chem.* **2009**, *284* (23), 15894–15902.
(100) Wood, J. D.; Gregory, N. G.; Hall, G. M.; Lister, D. Fat mobilization in Pietrain and Large White pigs. *Br. J. Nutr.* **1977**, *37* (2), 167–186.
(101) Gregory, N. G.; Wood, J. D.; Enser, M. E.; Smith, W. C.; Ellis, M. Fat mobilization in large white pigs selected for low backfat thickness. *J. Sci. Food Agric.* **1980**, *31* (6), 567–572.
(102) Vander Heiden, M. G.; Cantley, L. C.; Thompson, C. B. Understanding the Warburg effect: the metabolic requirements of cell proliferation. *Science* **2009**, *324* (5930), 1029–1033.

PR100693H